Your reference: wes-2025-115 Date: October 14, 2025

DTU Wind and Energy Systems DTU Risø Campus Frederiksborgvej 399 4000, Roskilde Denmark

Subject: Author's Response Wind Energy Science Journal Reviewers

Dear Reviewers,

Thank you for your constructive and detailed comments on our paper. Your feedback helped us significantly improve our manuscript. This document presents our reply to the comments raised and provides an overview of the changes we made. Responses to each comment are given in blue color, and related changes in the manuscript are given in red color. A marked-up version of the revised manuscript is also attached, where the removed portions are indicated by red strikethrough and added text is indicated by blue underlined text. Hence, we provide a clear and detailed response to your comments.

Sincerely,

Büsra Yildirim Nikolay Dimitrov Asger Bech Abrahamsen Athanasios Kolios

Enclosure(s):

- General remarks
- Response to Reviewer 1
- Response to Reviewer 2
- Marked-up version of the revised manuscript

Response to Reviewer 1

The paper investigates the potential for optimizing floating wind turbines (FWTs) through a novel twostep hybrid optimization framework. This framework introduces innovation by combining design space reduction with surrogate-based modelling to enhance computational efficiency.

In the first step, the design space is reduced by applying design constraints aimed at excluding infeasible solutions. During this phase, the design variable vector X_d (representing buoyancy column dimensions and floater radius) and the environmental condition vector X_e are defined. Additionally, analytical design constraints are introduced based on the floater's dynamic behaviour and overall geometric limitations.

In the second step, a surrogate model based on feedforward neural networks is trained using aero-hydroservo-elastic simulations. This surrogate model enables efficient evaluation of the system's dynamic performance, significantly reducing computational cost. The design space and environmental conditions are further refined using Latin Hypercube Sampling.

The framework is demonstrated using the UMaine VolturnUS semisubmersible platform coupled with the IEA 15 MW Reference Wind Turbine (RWT). The optimization design variables include the external column diameter and floater radius. The objective is to minimize the Levelized Cost of Energy (LCOE), subject to constraints related to ultimate loads, serviceability, and fatigue performance.

Comments and suggestions:

1. The introductory part on the differences between design approaches is interesting and relevant to the study. It is suggested to further expand that section and also add additional references.

Response: Thank you for your comment. We expanded that section, including discussions about conceptual modeling [3, 2] and frequency domain optimization [6, 7].

Revised Section: Introduction is modified with additional references and discussion about conceptual design and frequency domain models.

2. The method is overall interesting. However, claiming that it is general for FOWT is too pretentious as this stage since there are design variables in the rotor (especially large and very flexible ones) and in the coupling between the rotor and the floater/moorings that still need to be proven as feasible with surrogate models. It is recommended that the paper title and abstract more clearly convey the fact that the procedure is so far applied only to floater design (and also assuming only some of the design variables).

Response: Thank you for your comment. We agree with your suggestion. We modified the abstract and title to present it more clearly that we optimized the floater only.

Revised Section: Title and abstract are modified.

3. The authors should better clarify the criteria with which the constraints in Table 5 have been selected.

Response: Thank you for your comment. We have added a more detailed explanation about the selection of the design constraints in Table 5, including references for tower natural frequency [7], stability [1], and static mean pitch angle [5]. The remaining constraints are also explained in more detail. In addition to Table 5, we have included more details on the design constraint for the second part of the optimization, utilizing references for dynamic surge motion [7] and nacelle acceleration [4].

Revised Section: We have added the discussion to Section 3.1. below Table 5.Additional discussion is added above Table 10 in Section 3.6.

4. To enhance the impact of the study, it is suggested that the authors give an estimation of the saving in terms of computational cost with respect to a direct optimization using the complete model in the time domain. In other words, the reader should understand better why it is important to have the two steps separately and use the surrogate model then: how long did this process take, with respect to using the complete model in HAWC2, run for several DLCs and seeds with different geometries? Are we getting the same accuracy? Is it worth it in terms of cost vs. accuracy?

Response: Thank you for your comment. In our approach, we reduced the design space based on the constraints we have and then built a surrogate model in the reduced space. With this approach,

we only reduced the design of the experiment for our surrogate model, which means that if we build the optimization in a single step and then apply the analytical constraints, those designs would be infeasible (all analytical constraints are geometry/structure dependent). Hence, we would waste computational time running simulations on the infeasible space. In terms of creating design space, this would result in a cost reduction of approximately $89.4\,\%$. If we compare the computational cost of using a surrogate model instead of aeroelastic simulations within the optimization, this would result in a computational reduction of $98.72\,\%$. Without the surrogate model, approximately $1.6\,$ million simulations would need to be performed.

Revised Section: The discussion about the computational cost is included in the discussion.

5. A more critical discussion on the expected sensitivity of the results to the initial modelling choices, such as the selection of variables and constraints, would be valuable. Additionally, presenting the trends of key load responses in the optimized configuration compared to the baseline would help strengthen the analysis.

Response: Thank you for your comments. Additional simulations are performed with HAWC2 for the optimized design and the baseline case. We presented key load responses for the operational cases. Both designs show similar load trends.

Revised Section: Additional discussion is added to Section 4.2. Time Domain Design Evaluation for comparing key load responses of both designs.

Response to Reviewer 2

A Major Comments

1. The paper presents an interesting and promising optimization concept that aims to reduce the design space exploration of FOWTs for generating surrogate models to support design optimization. This is a valuable direction, and the approach has potential to be quite impactful.

Response: Thank you for your review and constructive comments. We are pleased to improve our paper using your suggestions and comments.

2. The most notable contribution seems to be the proposed two-step approach and the development of the surrogate model. At present, however, the details provided may not be sufficient for readers to fully understand or replicate the methodology. In particular, the rationale behind specific design choices and the interpretation of the optimization results could be expanded to improve clarity and accessibility.

Response: Thank you for your comments. To improve the clarity of our steps, we added additional details on design constraints for both steps, the design of the experiment (surrogate input) generation. We also extended the interpretation of optimization results.

Revised Section: We modified Section 3.1. Definition of Design Constraints, Section 3.5.1. Generation of the training dataset, Section 3.6. Second Step of the optimization, and Section 4. Results.

3. The computational cost of constructing the surrogate model is not fully described, apart from mentioning that a supercomputing cluster was required. More context here (e.g., runtime, resources, or scaling considerations) would help readers assess the feasibility of applying this approach in other settings. Relatedly, it would be helpful to know how the surrogate model itself (and the resulting optimal design) was verified.

Response: Thank you for your suggestions. We detailed the cost of surrogate training in terms of the reduction in the number of simulations for the optimization problem, rather than using the true model. More context about the computational cost is not included since the computational time also depends on the aeroelastic turbine simulation settings. For example, a simpler model with fewer structural nodes could be performed in a much shorter time. In our case, the whole database can be generated with 50 nodes within 1.5 days (Note that the nodes are not fully utilized for our simulations. It was used for other tasks on the cluster as well.). The parallelization of the time-domain simulation is not possible; therefore, each simulation runs independently. The surrogate model is verified using relevant error metrics, including R² values. For the validation/comparison of

the optimized design, key load responses are provided through high-fidelity aeroelastic simulations. For further design verification, additional simulations should be performed, including other load cases.

Revised Section: Details on the cost of the surrogate model are included in Section 5, and discussion and key load responses are included in Section 4.2.

4. The description of the high-fidelity database could be clarified further. For instance, it is not entirely clear how environmental and design-based samples were combined. Since this step appears central to constructing a reliable surrogate, additional details would strengthen the paper and improve reproducibility.

Response: Thank you for your feedback. The design variables and environmental conditions are combined in a way that eliminates any correlation between them. By doing this, we aimed to ensure that we build our surrogate model without any dependency between environmental samples and design variables. To create the DOE, we initially perform the first step of the optimization, where, based on the analytical constraints, we obtain the feasible design area. We obtain equations for the boundaries, and then later we use them to filter samples we obtained from the uniform distribution and the initial range of the design variables. After this step, the same number of environmental conditions is generated, and then both are combined/concatenated to create DOE.

Revised Section: Discussion about the generation of DOE and combining design variables and environmental conditions are added to Section 3.5.1.

5. The discussion of LCOE uncertainties is thoughtful. This raises the question of whether structural mass might serve as a more robust figure of merit with less uncertainty. Additionally, it would be useful to clarify whether (and how) AEP changes with the platform model.

Response: Thank you for your response. In our approach to the design optimization, we considered that the AEP is constant for each design. The reason why we used LCOE as the objective of our optimization is that it ensures a better metric for comparison to the reference design. The power curve used for the AEP estimation is computed for the reference design (UMaine floater with IEA 15 MW turbine). A more detailed LCOE estimation could be more beneficial at the farm level design, which could be the next step in this optimization framework. Considering our assumptions, here using LCOE serves similar to using structural mass within the optimization. We also computed AEP for the optimized design (85.74 GWh) and reference design (85.93 GWh) where optimized design has 0.2211 % less AEP which can be caused by the larger pitch angle of the optimized system.

Revised Section: We added the key load/response comparison for the optimized and reference designs, including power generation comparison in Section 4.2. Additionally, the LCOE values are included for reference and optimized designs.

6. The sensitivity study could benefit from additional explanation. For example, how should the reader interpret the results shown in Figure 9? What is the reference for the reported errors?

Response: Thank you for your suggestion. Here, in Figure 9, we conducted a sensitivity study to examine the effects of varying the number of wind and wave seeds, as well as the simulation length. To perform this, we run simulations with different combinations and then compare the results with the case involving six wind and three wave seeds for each simulation length. Therefore, our reference is the case with the highest number of seeds (Six wind and three wave realizations). The results of this sensitivity analysis are presented for three quantities of interest, including mooring line tension, tower base moment, and the thrust force. The reason we selected these outputs is to represent the loads on different subsystems of the FWT system, which are subjected to various driving mechanisms. Here, the reader should interpret these results in light of the tradeoff between computational cost and accuracy. Statistically, using more realizations can increase the accuracy of postprocessing; however, we may also lose information on the floater's low-frequency response if the simulation length is not sufficiently long. So using the results in Figure 9, the readers can select the tradeoff between different numbers of wind and wave realizations for obtaining accurate statistics for a selected simulation length.

Revised Section: Figure 9 is modified and placed closer to where it is referred. The discussion is expanded in Section 3.5.1.

7. Figure 6 appears to play an important role in reducing the design space, but its meaning is somewhat difficult to interpret. For example, are the shown samples infeasible? How do the subfigures (a)–(f) relate to each other, and what do the different colors indicate? Adding clarification to the caption or text would improve readability.

Response: Thank you for your comment. In Figure 9, the shown samples are infeasible, and the different colors in the subfigures represent different design constraints and infeasible designs when they are computed. From Subfigures a to f, it is shown how we can decrease the feasible space with respect to different design constraints. This is useful for having more information about the design.

Revised Section: Section 4.1. is modified to include a more detailed discussion about Figure 9 and subfigures.

8. The process for building a Latin hypercube sampling from the feasible design space is not currently described, but seems to be an essential step in the study. Including this would strengthen the methodological transparency.

Response: Thank you for your comments. We agree that giving those details would strengthen the transparency and increase reproducibility. We included relevant discussion in Section 3.5.1. considering your previous comment (Major comment 4).

Revised Section: Discussion about the sampling from the feasible design space is described, and relevant text is added to Section 3.5.1.

9. The discussion of the final design optimization and results could be enriched. For example: which constraints are active? Which design variables changed, and why? What impact did these changes have on cost and constraints? Providing this interpretation would help highlight the significance of the results.

Response: Thank you for your comments. We enriched the discussion about optimization results.

Revised Section: We modified the discussion at Section 4.1. for the first step and at Section 4.2. for the final optimization results.

B Minor Comments

1. The first sentence of the abstract highlights uncertainty, but this theme does not appear again later in the paper. A more consistent discussion might improve the narrative.

Response: Thank you for your suggestions. Currently, in our framework, we have addressed only environmental uncertainties, considering the full joint environmental distributions. Uncertainty propagation, including other uncertainties, can be included as further work. We modified the related section to include uncertainties in the discussion.

Revised Section: Discussion section is modified to include uncertainty related discussion.

2. The phrase "buoyancy column diameter" could be made clearer, as technically all columns provide buoyancy.

Response: Thank you for your suggestion. We replaced the "buoyancy column diameter" with the "outer column diameter".

Revised Section: Related text within the manuscript is modified.

3. Tables and figures are sometimes referenced far from where they appear in the text, which can disrupt the flow of reading.

Response: Thank you for your comment for improving flow. We improved the locations of the related figures. Figure 4 is moved closer to where it is referred.

Revised Section: Related figures are relocated within the text (Figure 4).

4. The definitions of design constraints could be presented more clearly. The g_i functions may not be necessary for readers, and plain language explanations might be more effective. Variable definitions should ideally appear in the captions if they are used within the tables (e.g., Tables 5 and 10). Additionally, the placement of these two tables feels quite far apart.

Response: Thank you for your suggestions. We added definitions and details on the design constraints. Additional details are discussed in Reviewer 1 Comment 3.

Revised Section: We have added the discussion to Section 3.1. below Table 5. Additional discussion is added above Table 10 in Section 3.6. Tables are relocated so that they are closer to where they are referred to. Captions for Tables 9 and 10 are modfied.

5. "System stability" appears in the constraints with only one citation and minimal explanation. More context would be helpful here.

Response: Thank you for your response. Additional details are added for system stability in the design constraints section.

Revised Section: Relevant text is added to Section 3.1 to give more details on the system stability.

6. The discussion of six random seeds is not entirely clear. Is this applied for each environmental case?

Response: Thank you for your comments. We gave more details about the six random seeds in your Major comment 6. In total, we have 3 wind and 2 wave seeds that are applied to each environmental case during the surrogate model input generation. Since our surrogate model is deterministic (each time we predict the same input with the same environmental conditions), we built our surrogate model based on the median of those random seeds for each environmental case.

Revised Section: We added more details in Section 3.5.1. for the random seeds discussion.

7. Table 6 lists several optimization algorithms, but it is not clear which one was actually used in the study. If only one is applied, it may be best to focus on that rather than listing all.

Response: Thank you for your comments. We removed Table 6. In our paper, we wanted to implement gradient-free algorithms, and that is why we summarized them and discussed why we selected COBYQA approach.

Revised Section: Table 6 is removed. More details are added about why gradient-free algorithms and why we selected COBYQA in Section 3.3.

8. For the DEL calculations, it would be valuable to explain the assumption that each sample is equally likely, as this may not be obvious to readers.

Response: Thank you for your suggestion. We modified the discussion about the DEL calculations and explained that our sample space is large enough to consider full joint probability distributions of each sample, and we don't need to scale them. Even if we increase our selected M value, the result for $DEL_{Lifetime}$ wouldn't change.

Revised Section: Section 3.5.1. is modified to explain our assumption about equally likely environmental conditions.

9. The distributions of the environmental parameters are not described. Were they fitted to metocean data? Including this information would be helpful.

Response: Thank you for your suggestion. The environmental parameters are fitted to the reanalysis data from the ANEMOC database within the HIPERWIND project [8]. The joint distribution covers 32 years of data. The underlying distributions for each environmental condition are presented in Table 6.

Revised Section: For better interpretation, the related section is modified further in Section 3.5.1 (Generation of the Dataset)

10. Section 3.6: the sentence beginning "SLS is defined as the maximum..." is difficult to parse and could be revised for clarity.

Response: Thank you for your suggestions. We agree with your suggestions and paraphrased the sentence.

Revised Section: We paraphrased the sentence beginning "SLS is defined as the maximum..." in Section 3.6. for clarity.

C Style Comments

1. Both "FOWT" and "FWT" are used; standardizing terminology would improve consistency.

Response: We agree about this inconsistency. The initial idea was to use FWT as the standard terminology.

Revised Section: "FOWTs" within the text are changed to "FWT".

2. Sideways tables can be challenging to read. If possible, reformatting them would enhance readability.

Response: Thank you for this suggestion. We reformatted the table for better readability.

Revised Section: Table 1 is reformatted for enhanced readability.

3. Figure labels should be consistent with the text size. At present, Figures 4–9 are difficult to read.

Response: Thank you for your suggestions. To improve the readability of our manuscript, we modified Figures 4-9.

Revised Section: Figures 4 - 9 are modified to improve consistency and readability.

References

- [1] A. Biran and R. López-Pulido. *Ship hydrostatics and stability*. Elsevier: Butterworth-Heinemann, Amsterdam, second edition edition, 2014.
- [2] M. Borg and H. Bredmose. D4.4 Overview of the numerical models used in the consortium and their qualification. 2015.
- [3] F. Borisade, J. Gruber, L. Hagemann, M. Kretschmer, F. Lemmer, K. Müller, D. Schliph, N.-D. Nguyen, and L. Vita. D 7.4 State-of-the-Art FOWT design practice and guidelines. Unrestricted, University of Stuttgart, Stuttgart, 2016.
- [4] M. Leimeister, A. Kolios, M. Collu, and P. Thomas. Design optimization of the OC3 phase IV floating spar-buoy, based on global limit states. *Ocean Engineering*, 202:107186, Apr. 2020.
- [5] D. Matha, F. Sandner, C. Molins, A. Campos, and P. W. Cheng. Efficient preliminary floating offshore wind turbine design and testing methodologies and application to a concrete spar design. *Philosophical Transactions of the Royal Society A: Mathematical, Physical and Engineering Sciences*, 373(2035):20140350, Feb. 2015.
- [6] A. Pegalajar-Jurado, M. Borg, and H. Bredmose. An efficient frequency-domain model for quick load analysis of floating offshore wind turbines. *Wind Energy Science*, 3(2):693–712, Oct. 2018.
- [7] N. Pollini, A. Pegalajar-Jurado, and H. Bredmose. Design optimization of a TetraSpar-type floater and tower for the IEA Wind 15 MW reference wind turbine. *Marine Structures*, 90:103437, July 2023.
- [8] E. Vanem, E. Fekhari, N. Dimitrov, M. Kelly, A. Cousin, and M. Guiton. A Joint Probability Distribution Model for Multivariate Wind and Wave Conditions. In *Volume 2: Structures, Safety, and Reliability*, page V002T02A013, Melbourne, Australia, June 2023. American Society of Mechanical Engineers.

Surrogate-Based Design Optimization of Floating-Wind Turbines Turbine Floater in Time Domain

Büsra Yildirim¹, Nikolay Dimitrov¹, Athanasios Kolios¹, and Asger Bech Abrahamsen¹ ¹DTU Wind and Energy Systems, Frederiksborgvej 399, DK-4000, Roskilde, Denmark

Correspondence: Büsra Yildirim (bysyi@dtu.dk)

Abstract.

Floating wind turbine (FWT) design involves higher costs and greater uncertainty than onshore or fixed-bottom offshore turbines due to low technology maturity, limited operational experience, and harsh marine environments; these factors have led to conservative design practices. To address these challenges, we introduce a novel two-step deterministic surrogate-based optimization framework that enables efficient time-domain design optimization for the floater subsystem of FWTs. In the first step, analytical design constraints are applied to refine the design space and establish a feasible region. In the second step, a surrogate model is trained on high-fidelity aero-hydro-elastic simulations, covering the reduced design space defined from step 1. During an optimization run, the surrogate model replaces computationally expensive direct time-domain analyses, capturing the dynamic response of the system with significantly reduced computational effort. This approach effectively balances model fidelity and computational cost, bridging the gap between conceptual and detailed design phases for floating wind structures. We demonstrate the framework on a semisubmersible platform floater (UMaine VolturnUS) coupled with the IEA 15 MW reference wind turbine, a representative large-scale FWT. Two primary design variables — the buoyancy of the floater, the outer column diameter and the overall floater radius, are optimized to minimize the levelized cost of energy (LCOE) of the system. The optimization incorporates global structural limit state constraints covering ultimate (ULS), fatigue (FLS), and serviceability (SLS) requirements to ensure the design's structural feasibility. The surrogate-assisted optimization yields a design that achieves a LCOE of 176.9 €/MWh, which is a 3.7 % reduction in LCOE relative to the baseline, with feasibility validated against all ULS, FLS, and SLS criteria. These results highlight the framework's potential to reduce FWT costs and improve design reliability by enabling time-domain optimization without excessive computational expense.

1 Introduction

Offshore wind energy has emerged as a key element in the global shift towards sustainable energy production, offering significant advantages in wind resource quality and availability compared to traditional onshore installations (Esteban et al., 2011). However, as development expands into deeper waters exceeding 60 meters, floating wind turbine (FWT) systems become indispensable, introducing unique design complexities (Europe, 2017). These floating structures must reliably withstand dynamic interactions from combined aerodynamic, hydrodynamic, structural, and control forces, presenting substantial engineering challenges. Despite their promising potential, current FWT designs face significant barriers, elevated costs, increased

uncertainty, and limited operational experience, largely stemming from the nature of floating offshore technology. Therefore, addressing these challenges through advanced optimization strategies becomes crucial (Backwell et al., 2024).

Design optimization of the engineering system has multiple steps, including preliminary design, conceptual design, and detailed design. Depending on the design stage, the problem definition of the optimization process and the tools used differ in terms of different modeling fidelities. In terms of floating offshore wind turbine systems, different model fidelities are used for each design process. Preliminary/conceptual design optimization procedures usually require simpler models. Such simpler models will not necessarily capture all relevant phenomena and will not be capable of evaluating all relevant limit states. Moving towards Borg and Bredmose (2015) presented the conceptual design procedure of FWTs, which starts with a parametric tool based on static stability, considering the cost of the structure. In this step, the selected design is analyzed further with the frequency domain tools for eigen-analysis, computation of response amplitude operators (RAOs), and estimation of the performance of the system for selected site conditions. Another difference within the conceptual design stage is the consideration of environmental conditions (Borisade et al., 2016), where the conceptual stage mostly focuses on extreme conditions, while a more detailed environmental assessment, including fatigue analysis and statistical assessment, is performed within the detailed design stage. Moving towards a more detailed design, considering all standard limit states will require more complex engineering models, and the computational time requires attention. A key point of attention regarding modelling fidelity is the trade-off between the frequency domain and time domain models.

The dynamics of FWTs require capturing the complex interaction of the system and the stochastic environment. Nonlinear time domain analyses are required to capture these complex interactions in the FWT dynamics, including aerodynamic, hydrodynamic, control, and structural dynamics (Hegseth et al., 2020). Simplified models can be implemented to explore the design space or conduct the conceptual design phase to obtain optimum solutions. To solve this problem, different approaches are implemented in the literature for different design phases and modelling approaches for FWTs are presented in Table 1.

40

50

Frequency-domain models require less computational time compared to time-domain models. Frequency-domain approaches are therefore widely preferred in literature for building simplified FWT models and solving design optimization problems in the conceptual design stage. In Karimi et al. (2017), design optimization in the frequency domain is carried out to explore a wide range of platform designs with three stability classes on a linearized 5 MW turbine, whilst a multi-objective genetic algorithm optimization problem is built considering tower top acceleration and the cost of the platform as design performance criteria. Hegseth et al. (2021) investigated the effect of environmental conditions and inspection strategies on long-term fatigue reliability and design optimization using a frequency domain model. From this work, it is concluded that environmental model uncertainties play a significant role in fatigue damage, particularly when uncertainties are included, resulting in a nearly constant damage reduction of approximately two-thirds along the tower and upper part of the platform. A Pegalajar-Jurado et al. (2018) developed a 4-degree-of-freedom (DOF) frequency domain tool which relies on higher fidelity models for aerodynamic and hydrodynamic loading. With their approach, the tower base moments were estimated with acceptable errors for the operational range of a 10 MW semisubmersible configuration. Later, this method is employed in (Pollini et al., 2023) for a gradient-based optimization of a 15 MW tetra spar floater, where they investigated the design of the floater, mooring lines, and tower design. Dou et al. (2020) extended this approach by including analytical gradients within the gradient-based design optimization of

Table 1. Modeling approach comparison Comparison of modeling approaches for floating wind turbines (FWTs).

Modeling	Approach
Advantages	Disadvantages
Frequency-Domain Models	Frequency-Domain Models
Computationally efficient (fast calculations) (Borg and Collu, 2015) Suitable for preliminary and conceptual design phases Enables rapid exploration of large design spaces Facilitates multi-objective optimization with reduced computational demand-	Assumes linear system behavior, limiting accuracy (Borg and Collu, 2015; Journée and Massie, 2001)
Suitable for preliminary and conceptual design phases	Underpredicts dynamic and nonlinear structural responses
Enables rapid exploration of large design spaces	Unable to reliably capture transient (Borg and Collu, 2015) and nonlinear interactions (e.g., memory effects) (Journée and Massie, 2001)
Facilitates multi-objective optimization with reduced computational demand	Necessitates application of safety factors due to inherent uncertainties (Pillai et al., 2018)
Time-Domain Models	Time-Domain Models
High accuracy in capturing nonlinear and transient structural responses	Significant computational expense (Borg and Collu, 2015)
Comprehensive representation of aerodynamic, hydrodynamic, structural, and control interactions (GL, 2018) Reliable fatigue (GL, 2018) and ultimate load estimations Appropriate for detailed design stages and verification purposes-	Significant computational expense (Borg and Collu, 2015) Require input data from frequency domain simulations (Borg and Collu, 2015)
Reliable fatigue and ultimate load estimations (GL, 2018)	Not directly practical for iterative design optimization processes (Pegalajar-Jurado et al., 2018)
Appropriate for detailed design stages and verification purposes	Computationally prohibitive for extensive parametric analyses or repeated optimization cycles
Surrogate-Based Hybrid Approach (Proposed)	Surrogate-Based Hybrid Approach (Proposed)
Effectively balances computational effort and modeling accuracy	Requires cautious training and validation of surrogate models
Enables high-fidelity time-domain analyses at significantly reduced computational cost via surrogate modeling and design space reduction with analytical constraints	Performance depends on the quality and representativeness of surrogate training data
Facilitates detailed structural optimization across multiple limit states (ULS, FLS, SLS)	Initial computational burden associated with generating surrogate model training datasets

FWTs is implemented in the frequency domain for a single objective design problem for fast evaluation of the conceptual design stage(Dou et al., 2020).

The next stage of the design optimization requires a detailed design procedure, including time domain simulations or higher fidelity tools. Time domain simulations can provide a more accurate estimation of the loads, but also have higher computational costs. Therefore, it is not directly possible to conduct time domain design optimization without simplifications or reduction in the load scenarios. Leimeister developed an automated design optimization framework (Leimeister et al., 2020a) for global limit states using Modelica and Dymola for an OC3 spar buoy (Leimeister et al., 2020b), resulting in almost a 24% reduction in structural mass of the spar compared to the reference OC3 Spar buoy design considered. In addition to the deterministic approaches, there are a few examples of reliability-based design optimization (RBDO) studies for FWTs in the literature. RBDO methods incorporate uncertainty information into the design process, ensuring simultaneously a safe, robust, and cost-efficient design. The first application of RBDO on FWTs for floater optimization combines a quadratic response surface approach and Monte Carlo simulations for RBDO execution, while considering uncertainties (Leimeister and Kolios, 2021). Cousin et al. (2022) developed a two-step procedure for time-dependent RBDO problems and applied it to the design of a mooring line system for a semisubmersible floater. Initially, they reformulated the design constraints using ergodic theory and extreme value theory and then performed optimization using adaptive Kriging. More detailed reviews on FWT design optimization can be found in (Ojo et al., 2021; Patryniak et al., 2022; Zhang et al., 2022).

Pillai et al. (2018) compared the time domain and frequency domain methods for the mooring line geometry, observing that the frequency-domain model was underpredicting mooring line Damage Equivalent Loads (DELs). This underprediction led to selecting infeasible designs, which demonstrates that the usage of the frequency domain models is not suitable without using safety factors. The limitations of the frequency domain approach stem primarily from treating the dynamic systems as linear, resulting in a linear relationship between body kinematic variables. Additionally, without including an impulse response function for the hydrodynamics, it fails to account for how past movements affect the current behavior and ignores the memory effects (Journée and Massie, 2001).

Surrogate models have the ability to map complex relationships, and are frequently used to replace complex numerical models. This includes models relevant for FWTs and their design process, such as models for load time series simulation and prediction of systems properties. In Singh et al. (2025), prediction of 10-minute DELs is performed using a probabilistic surrogate model (Mixture Density Network) to compute conditional statistics while utilizing uncertainties due to site conditions. With this approach, they also minimized the training cost due to random seed repetitions. Other areas for surrogate modeling usage on FWTs can be the prediction of system properties. Baudino Bessone et al. (2024) applied a tree-based ensemble method as a surrogate modeling (XGBoost) technique for the Radiation diffraction analysis to predict the hydrodynamic coefficients with a mean error of 7%

The selection of the objective function for the optimization problem might also change the outcome of the process. The life cycle cost or the levelized cost of energy, which is subject to many unknowns and uncertainties, should be considered an objective function for the structural optimization of wind turbine structures (Muskulus and Schafhirt, 2014). This is especially important in defining the cost reduction potential of the design optimization methodology.

Additional structural optimization recommendations for the FWT systems can be stated as modeling with a hierarchy of fidelities to select suitable details for the selected stage, defining/reducing the design driving load cases, and exploring the probabilistic design possibilities while reducing the uncertainties in the system (Muskulus and Schafhirt, 2014).

This work introduces a novel two-step hybrid optimization framework specifically developed for FWT design, effectively addressing critical gaps in existing approaches (Table 1), and increasing the modelling fidelity achievable within automated design optimization of floating wind systems. The primary innovation lies in the strategic combination of analytical constraints and surrogate modeling techniques within a structured deterministic optimization procedure. Initially, analytical design constraints are systematically applied to substantially reduce the design space, efficiently excluding infeasible configurations. Subsequently, surrogate models—carefully trained using high-fidelity aero-hydro-elastic simulations—are employed to replace computationally intensive direct time-domain simulations within this refined design space.

The paper is organized as follows: Section 1 introduces the motivation, establishes the context, and reviews previous studies on FWT design optimization, highlighting the necessity and challenges associated with time-domain simulations. Section 2 details the methodology, describing the generation of the initial design space, parameterization of the FWT system, and the numerical modeling approach. Section 3 elaborates on the design optimization procedure, including the selection and definition of the design variables, the formulation of objective functions and constraints, and the overall optimization steps. Within this, Section 3.5 specifically explains the surrogate modeling technique, detailing the dataset generation, sensitivity analysis to simulation seeds, and validation processes. Section 4 presents the optimization results, Section 5 provides a discussion interpreting these outcomes, and Section 6 offers concluding remarks and suggestions for future research directions.

2 Methodology

115 **2.1** Overview

105

110

125

The methodology followed in this paper has four main elements: generation of input space, computation of system properties, surrogate modeling, and design optimization. This is illustrated in Figure 1. The approach presented here can be applied to different turbine and floater types.

The design process begins with the **design of experiment**, where a specific floater concept is selected for the optimization. At this stage, key design variables (denoted collectively as \mathbf{X}_d) and relevant environmental conditions, \mathbf{X}_e are identified. Joint site-specific distributions for \mathbf{X}_e , are defined, and samples of the design variables \mathbf{X}_d are generated for the initial step of the design optimization. The augmented design vector is defined as $\mathbf{X} = [X_d, X_e]$.

Following this, the system properties for design configurations within the selected design space are computed. This involves evaluating initial design samples using analytical limit states to define the feasible design space. Once this space is identified, new samples of environmental variables X_e and design variables X_d are generated within the feasible region using the predefined distributions.

The next phase focuses on surrogate modeling. A high-fidelity training database is created using an aero-elastic simulation tool, which serves as input for training surrogate models $S_{Li}(X_e, X_d)$. This database is constructed for the normal operation

of the wind turbine. Feedforward neural networks are trained to map environmental conditions and design variables for each quantity of interest (QoIs), including system responses, loads, and damage equivalent loads (DELs).

Finally, the last step is **design optimization** considering global limit states. In this phase, the surrogate models trained in the previous step are used to perform optimization. Samples are generated for the environmental variables X_e for operational conditions, and the surrogate models are used to predict the QoIs for each limit state. The limit states computed are Ultimate Limit State (ULS), Serviceability Limit State (SLS), and Fatigue Limit State (FLS). For FLS, Monte Carlo simulations are performed as means of numerically integrating short-term fatigue damage estimates to obtain the lifetime fatigue damage.

2.2 Description of the Reference FWT Design

130

135

145

150

155

160

The semisubmersible UMaine floater (Allen et al., 2020) is selected as the FWT reference design, due to its technical advantages, publicly available information, and commercialization preference for the semisubmersible concepts. The UMaine semisubmersible floater (see Figure 2 and Table 2) selected in this study is characterized by a steel substructure composed of three buoyancy outer columns connected by rectangular pontoons, and a central column supporting the wind turbine tower base. This configuration provides substantial hydrodynamic stability due to its relatively large waterplane area, which effectively limits platform motions, enhancing structural stiffness and robustness against wave-induced loading. Furthermore, the semisubmersible design provides efficient tow-out and installation processes due to its moderate draft requirements, reducing associated logistical and installation expenses. However, key disadvantages include its relatively complex structural design, potentially higher initial manufacturing and maintenance costs compared to simpler concepts such as spars, and vulnerability to fatigue due to significant wave interaction with the pontoons, which requires careful fatigue load assessment during design optimization. The reference design includes solid and water ballast. In this work, only solid ballast is preferred.

Semisubmersible platforms have increased waterplane area compared to spar platforms, contributing to better hydrodynamic stability, structural stiffness to resist wave loads, and greater towability, which ensures more straightforward installation and decommissioning properties (Jiang, 2021). Additional advantages include low draft requirements and lower mooring costs (Ojo et al., 2022).

The semisubmersible platform is coupled with an IEA 15 MW turbine (Gaertner, 2020) with a modified tower from the Hiperwind_HIPERWIND project (Capaldo et al., 2021b) and a controller with the tower top velocity feedback controller previously tuned for the reference design. The controller with tower top fore-aft velocity feedback loop is designed to prevent the floater pitch instability problem (Meng et al., 2023). This method is developed as an alternative to detuning the controller to prevent pitch instability and demonstrated by an experimental campaign for Tetra spar type FWT. For controller details, please see (Meng et al., 2023).

The reference design is adapted to a site in South Brittany at 150 m water depth with three equally spaced catenary mooring lines. The South Brittany site is selected due to having strong and consistent Atlantic winds. The water depth is also suitable for floating wind turbine installation while being relatively close to the shore. This site is also selected within the HIPERWIND project (Capaldo et al., 2021a) for FWT analysis, and currently, there is an offshore wind farm planned in the region.

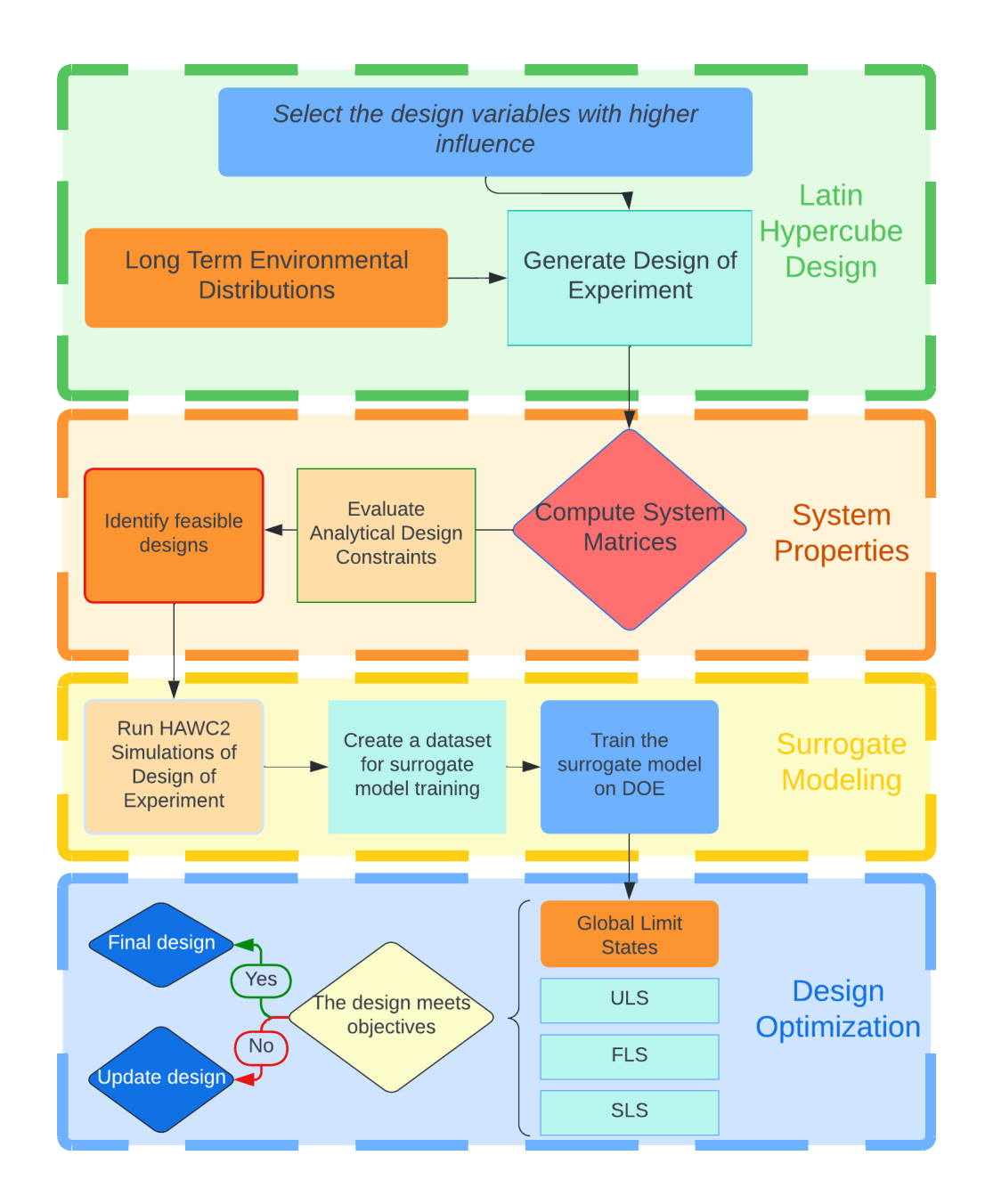


Figure 1. Flowchart of the methodology

Table 2. System Properties of the Floating Offshore Wind Turbine. Modified from (Allen et al., 2020)

Parameter	Units	Value
Turbine Rating	MW	15
Hub Height	m	150
Excursion (L, W, H)	m	90.1, 102.1, 290.0
Freeboard	m	15
Draft	m	20
Total System Mass	t	20,093
Tower Mass	t	1,263
RNA Mass	t	991
Mooring System	_	Three-line chain catenary

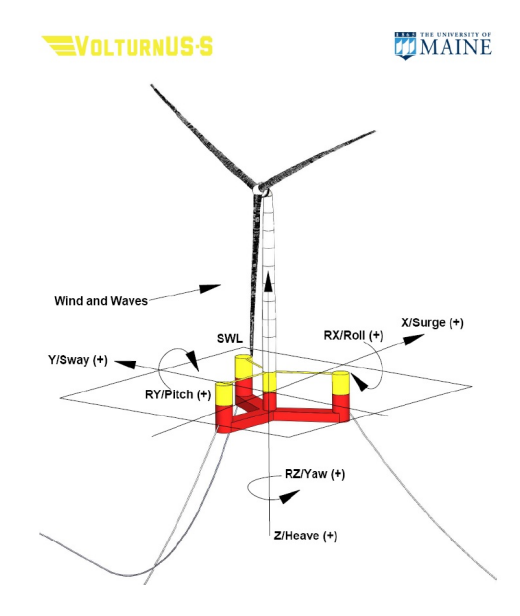


Figure 2. Selected reference design case (Allen et al., 2020)

2.3 System Parameterization and Modeling

System parameterization is utilized in both steps of the optimization process. In the first step, the system properties, such as mass, stiffness, and natural frequencies, are computed for each design with respect to the current values of the design variables \mathbf{X}_d (see Table 3 for an overview of all variables in \mathbf{X}_e and \mathbf{X}_d). In the second step of the optimization simulation, additional parameters are derived.

For the hydrodynamic modeling, the selected reference floater design case is parameterized to generate the mesh used for computing the hydrodynamic coefficients of the floater. The mesh generation is automated using gmsh (Geuzaine and Remacle, 2009), considering the given design interval, and the mesh size is selected based on previous studies (See (Yildirim et al., 2024; Yildirim and Dimitrov, 2024)). The Boundary Element Method solver HAMS / pyHAMS (Liu, 2019) calculates hydrodynamic coefficients. The equation of motion is solved in the time domain, and irregular waves are generated using the JONSWAP spectrum according to the parameters selected in the DOE creation process. The wind turbine model of the IEA 15 MW turbine (Gaertner, 2020) is implemented in HAWC2. An overview of the tools used is presented in Table 4.

2.4 Selection of the Design Variables

170

The contribution of the substructure cost to the total capital expenditure (CAPEX) of the FWT system is significant. For instance, a reference 6.1 MW turbine has around 27 % CAPEX contribution from substructure and foundation (Stehly and Duffy, 2021). Reducing the traditional factor of safety for the FWT systems can be one method to decrease this cost contribution. To ensure this, the floater is selected as the component for the design optimization study. Other system components, such as

Table 3. Overview of the design and environmental variables

Variable	Description
U_{\sim}	10 minutes averaged wind speed [m/s]
$\underbrace{Yaw_{mis}}$	Yaw misalignment [°]
$\overset{\sigma_u}{\sim}$	Standard deviation of the wind speed [m/s]
$\stackrel{H_s}{\approx}$	Significant wave height [m]
W_{dir}	Wave Direction [°]
$T_{\mathcal{R}}$	Peak Wave Period [s]
$\stackrel{R_{f_{\sim}}}{\approx}$	Flaoter Radius [m]
D_{buou}	Outer Column Diameter [m]

Table 4. Overview of tools for the framework

Tool	Purpose/Function	Suitability	
Gmsh	Automated finite-element mesh	Efficiently produces repeatable, high-quality meshes	
	generation for floater geometry.	necessary for accurate hydrodynamic modeling in iter-	
		ative design optimization.	
(py)HAMS	Boundary Element Method	Precisely calculates hydrodynamic coefficients, essen-	
	solver for hydrodynamic coef-	tial for modeling floating structure dynamics.	
	ficient calculation.		
HAWC2	Aero-elastic simulation of the	Accurately simulates coupled aero-hydro-elastic dy-	
	FWT dynamics.	namic responses, necessary for reliable assessment of	
		structural loads, responses, and fatigue.	
-			

the tower, turbine, and station-keeping system, remain unchanged. Only the floater's design variables are changed during the optimization process.

The design variables considered in this study are defined based on a design evaluation and sensitivity analysis study for the floater design (Yildirim et al., 2024) conducted by the author. According to this study, floater radius and buoyancy outer column diameter are the design variables with the highest effect on the system response and the cost compared to other variables, such as tower base column diameter, draft, and the mooring line length. Regarding cost comparison, the outer column diameter has

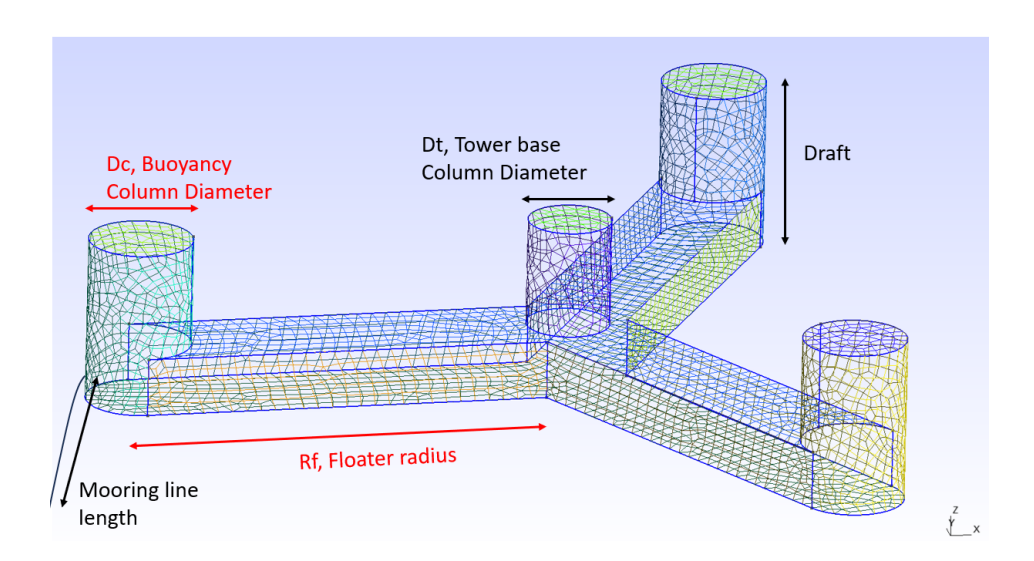


Figure 3. Visualization of selected design variables. Regenerated from (Yildirim et al., 2024).

190

195

200

the highest contribution. Therefore, for the design optimization study, those two variables are selected for further design space exploration. Different from the reference design, the ballast of this system is taken as solid ballast material only and is adjusted based on the floater design and buoyancy of the total system.

To keep the same floater class (e.g., semisubmersible), the design interval is defined such that designs with very short and long drafts are eliminated from the initial design of experiment (DOE) screening. Finally, the design variables vector is defined as: $\mathbf{X_d} = \{x_1, x_2\}$ where x_1 is the buoyancy outer column diameter and x_2 is the floater radius. Selected design variables are presented in Figure 3 in red.

Overview of the design and environmental variables Variable Description U 10 minutes averaged wind speed m/s Yaw_{mis} Yaw misalignment $^{\circ}\sigma_u$ Standard deviation of the wind speed m/s H_s Significant wave height m W_{dir} Wave Direction $^{\circ}T_p$ Peak Wave Period s R_f Flaoter Radius m D_{buoy} Buoyancy Column Diameter m

In this study, we focus specifically on two key design variables - floater radius and buoyancy outer column diameter - due to their substantial influence on system response and cost, as identified by prior sensitivity analyses. However, the optimization framework presented here is flexible and can readily accommodate additional variables in future studies. Variables such as pontoon geometry, draft depth, ballast distribution, structural thickness, and mooring configuration can be integrated into the framework to facilitate more comprehensive design explorations. Such an extension would enable deeper insights and broader optimization possibilities, particularly in detailed design phases where more complex interactions among multiple design parameters must be accurately captured and evaluated.

2.5 Definition of the Objective Function: LCOE

The optimization problem in this work is defined as a single-objective optimization problem. The objective function is formulated to minimize the levelized cost of energy (LCOE). By incorporating CAPEX, operational expenditures (OPEX), and energy production over the system lifetime, LCOE enables a comprehensive assessment of design trade-offs, directly linking technical design decisions to economic outcomes. This approach facilitates transparent comparisons among competing FWT configurations and provides a robust basis for evaluating the practical impact of design optimizations. However, it should be acknowledged that uncertainties in cost estimation, market fluctuations, model uncertainties, and variable environmental conditions may affect the precision of LCOE calculations. Future studies on integrating probabilistic or uncertainty-based assessments to further enhance decision-making robustness can increase the accuracy of the LCOE computations.

3 Design Optimization

205

210

225

230

The two steps in our proposed optimization approach make use of a common set of design variables \mathbf{X}_d and environmental variables \mathbf{X}_e , as defined in Section 2. The remaining elements of the optimization problem include design constraints (analytical constraints evaluated in step 1, and dynamic limit state constraints used in step 2), an optimization algorithm, and an objective function. All these are defined in the following.

3.1 Definition of the Design Constraints

The design constraints can be grouped in into three types:

- 1) Analytical design constraints based on steady-state floater characteristics, motion, and stability limits;
- 2) Design geometry constraints based on production and concept limits for the floater;
- 3) Global dynamic limit states (SLS, ULS, FLS as required by a standard design load basis) as well as maximum allowable motion limits

All constraints are defined as hard constraints, which refer to strict conditions that must be satisfied for a solution to be considered feasible. From the list above, the first two constraint groups are evaluated analytically during the first step of the optimization process, while the last group is computed with time domain simulations and surrogate modeling as part of step 2.

The design constraints used in the first optimization stage are listed in Table 5. Analytical design constraints are given specified by $g_1(X)$ to $g_6(X)$, representing which represent limits on natural frequencies, stability, and the static pitch angle under rated wind speed. $g_7(x_1)$ and $g_8(x_1)$ represent lower and upper geometric boundaries for buoyancy outer column diameter (x_1) , while $g_9(x_2)$ and $g_{10}(x_2)$ are the floater radius (x_2) lower and upper boundaries, respectively.

Design constraints for the first part of the optimization are selected to eliminate infeasible designs before running simulations, thereby reducing computational cost. The natural frequency constraints, as surge $(g_1(X))$ and pitch $(g_2(X))$ and $g_3(X)$, are selected to prevent resonance due to load frequencies resulting from wave loads and controller behavior. For the tower,

Table 5. Design Constraints for the First Stage of the Optimization where ω_1 is the surge natural frequency, ω_2 is the pitch natural frequency, ω_3 is the tower natural frequency of the system. θ_{static} is the static pitch angle under thrust force at rated wind speed. x_1 and x_2 are our design variables where x_1 is the floater radius length and x_2 is the outer column diameter.

Constraint	Expression	Description	Unit			
	Analytical Design Constraints					
$g_1(X)$	$\omega_1 - 0.01$	Surge Natural Frequency	Hz			
$g_2(X)$	$\omega_2 - 0.035$	Pitch Natural Frequency (Lower Bound)	Hz			
$g_3(X)$	$0.025 - \omega_2$	Pitch Natural Frequency (Upper Bound) (Pollini et al., 2023)	Hz			
$g_4(X)$	$\omega_3 - 0.469$	Tower Natural Frequency	Hz			
$g_5(X)$	-system stability	System Stability (Pollini et al., 2023)	-			
$g_6(X)$	$\theta_{ m static} - 5$	Static Pitch Angle (Pollini et al., 2023)	0			
	Constraints for the Design Variables					
$g_7(x_1)$	$25 - x_1$	Floater Radius Lower Boundary	m			
$g_8(x_1)$	$x_1 - 80$	Floater Radius Upper Boundary	m			
$g_9(x_2)$	$5.0 - x_2$	Buoyancy Outer Column Diameter Lower Boundary	m			
$g_{10}(x_2)$	$x_2 - 25.0$	Buoyancy Outer Column Diameter Upper Boundary	m			

the natural frequency constraint is selected for stiff-stiff tower design where the tower's natural frequency should be placed above the 3P region (Pollini et al., 2023). The hydrostatic pitch stability of a floating body can be expressed in terms of the hydrostatic pitch restoring stiffness, and it should be positive for the floater to be stable. This stability constraint can be explained by the stability analysis of floating bodies, which considers the center of gravity, buoyancy center, and metacenter (Biran and López-Pulido, 2014). Static mean pitch angle is constrained with a strict 5 °criteria at rated wind speed to ensure stability and efficient power production (Matha et al., 2015).

3.2 Computation of Analytical Design Constraints

235

245

The first step of the design optimization process involves computing the system matrices, including mass and stiffness. The total stiffness matrix includes the contribution from the structure, the hydrostatic stiffness matrix, and the mooring stiffness matrices.

After computing the system matrices, the generalized eigenvalue problem is solved to obtain the system's natural frequencies. Mode partitioning is applied to differentiate contributions from each degree of freedom (DOF) to rank the different 'designs' natural frequencies. The system's stability is formulated using the total pitch stiffness of the structure. The results of the first design optimization part are presented in Figure 6 and Section 4.1 in detail.

3.3 Optimization Methodology

250

255

260

265

270

Optimization algorithms can be defined as two main categories: gradient-based and gradient-free algorithms. Gradient-based algorithms leverage derivative information to rapidly converge towards local optima but require smooth, differentiable functions, whereas gradient-free algorithms are more robust for complex, non-smooth, or discontinuous problems but typically converge more slowly and require more function evaluations.

The present work employs the Some of the gradient-free optimization algorithms are inspired by nature. For example, the genetic algorithm (GA) is a population-based metaheuristic algorithm that is effective for exploring large, multimodal, and nonlinear search spaces (kus, 2012). Particle swarm optimization (PSO), which is inspired by the social behavior of birds Kennedy' and Eberhart (1995), is effective for high-dimensional problems. Constrained Optimization by Linear Approximations (COBYLA) uses linear approximations to handle nonlinear constraints without requiring gradient information (pow, 1994) and can not handle variable boundaries directly. Constrained Optimization by Quadratic Approximations (COBYQA) (Ragonneau, 2022) is an improved version of the COBYLA algorithm, which constructs quadratic models of the objective and constraints to solve constrained nonlinear problems (Ragonneau, 2022).

The present work employs the COBYQA (Ragonneau, 2022) algorithm, which is a model-based derivative-free algorithm for nonlinear constrained optimization problems. COBYQA is a trust region approach and focuses on improving the local solution around the current iterate. COBYQA is particularly suitable for this study because it combines the strengths of gradient-free optimization with the efficiency and local accuracy typically associated with gradient-based methods. Specifically, it builds local quadratic approximations of the objective and constraint functions, enabling it to efficiently handle constrained nonlinear optimization problems without requiring explicit derivatives. This makes COBYQA especially effective for computationally expensive problems, such as surrogate-based design optimizations of floating wind turbines, where derivatives might be challenging to compute, yet accuracy, convergence reliability, and computational efficiency remain critical.

The details of the optimization algorithm can be found in (Ragonneau, 2022). COBYQA resulted in better convergence in our problem and had lower computational time compared to COBYLA, a similar, earlier version of the algorithm. A short overview of all optimization algorithms considered is given in Table ??. The generic optimization problem can be summarized as follows:

Minimize:
$$f(\mathbf{x})$$
 Subject to: $g_i(\mathbf{x}) \leq 0, \quad i=1,2,\ldots,m$
$$x_k^{(\mathrm{lower})} \leq x_k \leq x_k^{(\mathrm{upper})}, \quad k=1,2,\ldots,n$$

Where $\mathbf{x} = [x_1, x_2, ..., x_n]^T$ is the vector of design variables, and for our case, there are two design variables and six environmental variables. For details, see Section 2.4. $f(\mathbf{x})$ is the objective function to be minimized, in our case represented by the LCOE (the computation of LCOE is described in the following Section 3.4). $g_i(\mathbf{x})$ are the inequality constraints and

 $x_k^{\text{(lower)}}$ and $x_k^{\text{(upper)}}$ are the lower and upper bounds for each variable. The optimization problem described in this work does not include any equality constraints.

Gradient-Free Optimization Algorithms Algorithm Description COBYQA Derivative-free trust-region method that constructs quadratic models of the objective and constraints to solve constrained nonlinear problems (Ragonneau, 2022). COBYLA Uses linear approximations to handle nonlinear constraints without requiring gradient information (pow, 1994). Can not handle variable boundaries directly. Genetic Algorithms (GA) Population-based metaheuristic inspired by natural selection; effective for exploring large, multi-modal, and nonlinear search spaces. (kus, 2012) Particle Swarm Optimization (PSO) Population-based algorithm, which is inspired by the social behavior of birds. (Kennedy' and Eberhart, 1995) It is effective for high-dimensional problems.

3.4 Methodologies for Estimating LCOE under FWT Design Optimization

3.4.1 Computation of LCOE

280

285

290

295

305

LCOE is useful as an assessment tool for project viability as it provides a standard comparison by an economics-related metric. The LCOE by definition includes costs related to capital investments, operation, maintenance, and other project-related costs (Eq. 1). Estimation of LCOE for different FWT concepts, such as semisubmersible, tension leg platform (TLP), and spar, is compared in (Myhr et al., 2014), where they concluded that a floating wind array 100 km offshore has an LCOE range of 82 - 236.7 €/MWh. They also identified the cost-driving aspects in two categories: discount rate, distance to shore, water depth, and farm size are considered predictable factors, while load factor, variation of the steel price are the uncertain factors with high effects on the LCOE. In another study, different deployment sites and three floater concepts are considered for a 500 MW floating offshore wind farm where the final LCOE values are estimated between 67 - 135 €(Lerch et al., 2018). They also highlighted that manufacturing-related costs highly influence the LCOE, such as the cost of the turbine, floater, and the station-keeping system, which states the importance of a cost-optimized design.

LCOE can be analyzed by different fidelities. This work prefers a simplified approach to compute the LCOE as an objective function. The LCOE is computed as defined in Equation 1.

300 LCOE =
$$\frac{\sum_{t=1}^{T} \frac{\text{CAPEX}_t + \text{OPEX}_t}{(1+w)^t}}{\sum_{t=1}^{T} \frac{E_t}{(1+w)^t}}$$
(1)

Where $CAPEX_t$ is the capital expenditure in year t, $OPEX_t$ is the operational expenditure in year t, E_t is the electricity generation in year t, w is the discount rate which is 8 - 12 % for offshore wind projects (Myhr et al., 2014), T is the lifetime of the system. Here, the LCOE is computed based on the material mass of the system. Operational costs are included as a percentage of the material cost. Due to early-stage floating wind markets, uncertain regulatory environments, and emerging FWT technology, the discount rate is selected as 12% to account for uncertainties and risks. For a typical offshore wind project, the lifetime of the structure is defined as 20-25 years. In this work, 25 years is selected as the lifetime of the project. For the

computation of LCOE, the turbine price is taken from the (Agency, 2016). Details of the Annual Energy Production (AEP) computation are presented in the next section.

3.4.2 Computation of AEP

During the lifetime of the structure, the AEP is assumed to be constant; therefore, yearly wind resource variability is not considered. The probability distribution of the short-term (ten-minute) average wind speed is modelled as Weibull distributed, with the distribution parameters A_w and k_w (scale and shape parameters respectively) derived from the environmental data discussed in Section 3.5.1. The Weibull distribution is selected for wind speed modelling as it is widely adopted in practice when modelling wind energy potential (Ucar and Balo, 2010). The AEP computation formula is given in Equation 2:

315 AEP =
$$\int_{0}^{\infty} F(u)P(u) \cdot du$$
 (2)

where u is the ten-minute average wind speed, F(u) is the PDF of the Weibull distribution for the site, and P(u) is the power curve computed for the reference FWT considered in this work.

The AEP is calculated through detailed time-domain aero-elastic simulations performed with HAWC2, using inputs such as realistic turbulent wind fields, turbine control settings, and structural characteristics of the turbine and floater. These simulations yield power production and structural response outputs across operational wind speeds, which are subsequently integrated with site-specific wind distributions to estimate the annual energy yield. The annual energy production for a single turbine is calculated using Equation 2. AEP calculation is performed for two cases: 1) no turbulence and no wind shear, and 2) a turbulent case with IEC (International Electrotechnical Commission) NTM (Normal Turbulence Model) turbulence representative of the South Brittany Site. Six random seeds are considered for each case, to consider realization-to-realization variability due to turbulence as prescribed by the IEC 61400 design guideline (iec, 2019). The computed AEP values are 82.31 GWh for the no-turbulence case and 81.45 GWh for the IEC NTM turbulence model, which is 1.05 % lower than the former. This difference arises in the shoulder region of the power curve, where turbulence fluctuations at wind speeds close to rated will cause wind speed dips that lead to lower power production, but cannot be compensated with similar production peaks as the turbine hits is nominal power limit when the wind speed increases.

330 3.5 Surrogate Modeling Approach

325

335

The classical application of surrogate models is as a computationally efficient replacement of a high-fidelity tool in modelling a relationship between an input (design variable or environmental variable) and an output Quantity of Interest (QoI). This approach is applied in the present study in two ways. Firstly, wherever feasible, surrogate models are used to provide a direct mapping between design variables and output QoIs. This is applicable to the SLS and ULS limit states which are defined as single events. Computing the FLS limit state requires an additional step, where the lifetime fatigue damage is computed from short-term DEL quantities through a numerical integration. In this case, the surrogate model is trained to estimate short-

term DELs and the numerical integration is introduced as an additional step. The need of numerical integration increases the computation requirements and necessitates that a highly efficient surrogate model is chosen.

In further consideration to the choice of surrogate, making gradient-based design optimization feasible requires at least the first-order differentials, a requirement which is satisfied by either polynomial-based models or a neural network with a continuous activation function (Dimitrov and Natarajan, 2021). In addition to this, gradient-enhanced surrogate modeling techniques can also increase the accuracy and computational efficiency of the optimization problem (Yamazaki et al., 2010).

Although neural networks may not be ideal for gradient-based optimization due to the tendency to overfit (which creates local extremes), they are very computationally efficient and have been found to be suitable for site-specific load estimation, considering time, accuracy, and convergence, particularly in a small sample space (Schröder et al., 2018). The requirement of high computational efficiency (in order to facilitate computation of FLS) and the availability of efficient gradient-free methods such as COBYQA, leads to the choice of feedforward neural networks (FNN) as surrogate models.

3.5.1 Generation of the Training Dataset

340

350

355

360

365

This paper benefits from training a site-specific surrogate model. The inputs include six environmental variables, including wind speed (U), wind direction (U_{dir}) yaw misalignment (Yaw_{mis}) , standard deviation of the turbulence (σ_u) , wave height (H_s) , wave direction (W_{dir}) , wave peak period (T_p) and two design variables as floater radius (R_f) and buoyancy outer column diameter (D_{buoy}) . As the training dataset has significant importance for the quality of the surrogate model and optimization output, the design of experiment (DOE) generating the inputs is carefully defined to fill the input domain evenly.

A Latin Hypercube Sample (LHS) is generated over the space $X = [X_e, X_d]$. The space-filling properties of the LHS design typically result in a more accurate trained model (Zhang and Dimitrov, 2024). The joint distribution of environmental conditions is modelled as a series of conditionally dependent variables using the Rosenblatt transformation (Rosenblatt, 1952), thus ensuring the correlation between variables is properly accounted for. The boundaries for the design variables are defined considering the operation limits of the turbine and the floater stability class limitations. The joint environmental distributions for the surrogate model training are defined based on the site conditions in South Brittany (Vanem et al., 2023) using hourly data from the ANEMOC database containing 32 years of reanalysis data (Forum, 2016). The six variable joint distributions previously defined are modified to represent the Vanem et al. (2023) fitted a multivariate joint distribution to the site conditions, where the wind speed distribution is modeled as a hybrid model of Weibull - Generalized Pareto Distribution (GPD) for a better representation of extremes. This six-variable joint distribution is adapted in our work with focus on the range of the turbine's operational conditions. Instead of the hybrid Weibull and generalized Pareto distributions Weibull-GPD defined in (Vanem et al., 2023) for the wind speed, only a Weibull distribution is used, as our interest is only in the operational wind speed rangeand resulted, and the resulting environmental condition pairplots are presented in Figure 4. The variable sequence in the joint conditional distribution is defined as in (Vanem et al., 2023):

$$f_{U,\sigma_{U},HS,TP,\theta,\beta}(u,\sigma,h,t,\theta,\beta) = f_{U}(u)f_{\sigma_{U}|U}(\sigma|u)f_{Hs|U}(h|u)f_{Tp|Hs}(t|h)f_{\theta|U}(\theta|u)f_{\beta|U}(\beta|u)$$

$$(3)$$

It should be noted that the range given for the design variables here represents the initial design space before the surrogate training, and it is used for the second step of the optimization problem. For the *U* values, the turbine operational range is preferred, and the limit states are also computed considering this operational range.

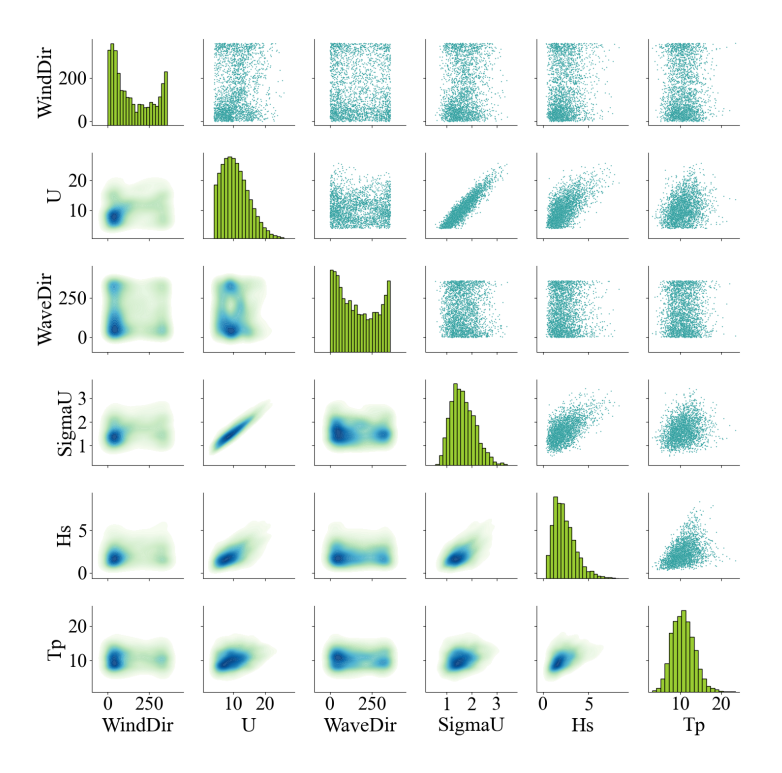


Figure 4. Environmental conditions for the normal turbulence model. Figure is regenerated from (Vanem et al., 2023) considering the changes in wind speed distribution.

For the surrogate model training, 3400 input sets are created based on the boundaries distributions listed in Table 6. This number is selected as appropriate when considering the design space coverage and computational efficiency. The DOE space is defined as an eight-dimensional Latin hypercube in normalized space. After generating the sample space, the normalized samples are converted back to physical space, taking into account the boundaries discussed. During sample generation for the DOE, environmental distributions and design variables were considered separately to ensure that design variables and environmental conditions are not dependent on each other. For sampling the design variables, initially, uniform distributions are defined based on the design variable boundaries. After performing the first part of the design optimization, feasible design

375

variable boundaries are fitted by binning the variable range and then filtered to obtain a feasible space. The same number of environmental conditions are sampled and then combined.

Table 6. Input features for the surrogate model

380

385

390

Table 7. Output features for the surrogate model

			~~~~		
Variable	Distribution		Limit	Quantity of Interest	Unit
$U_{\sim}$	Weibull		<b>State</b>	<del></del>	~~~
&~	Weldun				[ <u>m</u> ]
$Yaw_{mis}$	Uniform		SLS	Surge	
$\overset{\sigma_u}{\sim}$	Log Normal			<u>Pitch</u>	[°]
$H_{s_{\infty}}$	Weibull	~~		Tower Top Acceleration fa	$[m/s^2]_{\sim}$
$W_{dir}$	Von Mises			Tower Top Acceleration ss	$[m/s^2]_{\sim}$
****			ULS		[kN]
$T_{\mathcal{R}}$	Log Normal			Pontoon Bending	
~K	L Service Control of the Control of		FLS		[Mpa]
$R_{f_{\sim}}$	Uniform			Mooring Line 1 DEL	7000
~~~	~~~~				[Mpa]
D_{buoy}	Uniform			Mooring Line 2 DEL	

Time domain simulations are performed with the Hawe2-HAWC2 tool (Horizontal Axis Wind Turbine Simulation Code 2nd Generation (Bischoff Kristiansen, 2022)), using six random seeds per sample point, three for the wind turbulence and two for the waves. This results in a total of 20400 Hawe2-HAWC2 time-domain simulation data points. The resulting 20400 time series are post-processed to obtain the loads, responses, and DELs on the structure, which are summarized in Table 7. The 90 % quantiles of the time series are used to further assess the ULS, to capture the high load/response of the system without being overconservative. The short-term DELs are computed for tower base, mooring lines, and blade roots mooring lines by applying rainflow counting and the Palmgren-Miner's rule (iec, 2019) as in eq. Equation 4 below, where the S_i is the load/stress amplitude of a number of cycles n_i in the i^{th} bin, and m is the Wöhler exponent. The relationship between stress amplitudes and number of cycles to failure is derived from a standard SN curve where $N = QS^{-m}$. n_{ref} is the number of equivalent cycles over a reference period (e.g., setting n_{ref} to 600 for a 10-minute simulation results in 1 Hz-equivalent loads), and K is the total number of bins for DEL computation.

$$S_{eq} = \left[\frac{\sum_{i=1}^{K} n_i S_i^m}{n_{ref}}\right]^{\frac{1}{m}} \tag{4}$$

$$DEL_{Lifetime} = \left[\frac{N_{Lifetime}}{n_{ref}M} \sum_{i=1}^{M} S_{eq,i}^{m} \right]^{\frac{1}{m}}$$
 (5)

Lifetime DEL is estimated by direct sampling from the joint environmental probability distribution and obtaining surrogate model responses $S_{eq.i}$. The DEL summation is done using Equation 5, following the same notation as in Equation 4. Additional variables are defined as follows: $N_{Lifetime}$ is the total number of short-term periods over the lifetime of the system, n_{ref} is the number of cycles for the 1 Hz equivalent simulation length and M is the number of different environmental conditions used to compute $DEL_{Lifetime}$. M is defined with a convergence studyconsidering different numbers of environmental conditions, and it is selected as , where we computed $DEL_{Lifetime}$ for different values of M. Convergence was achieved after 50000 samples.

395

400

405

410

420

425

The DELs are estimated only for the operational range of the turbine. Note that Equation 5 holds when the lifetime DEL are computed by drawing a number of random samples equal to the total number of short-term periods corresponding to the operational life of the system (i.e., the computation effectively simulates the entire lifetime) At this sample size, convergence means we can conclude that the sample is representative enough of the full design space, and we can consider that each environmental condition sample has equal weight. Therefore, there is no need for further scaling of environmental conditions based on their joint probabilities. This approach is convenient as it does not require probability weighting (each Monte Carlo sample is assumed equally likely), but it requires an efficient surrogate model in order to be computationally feasible. The DELs are estimated only for the operational range of the turbine. The DEL computation makes use of an SN curve with an intercept of $Q = 6.0 \cdot 10^{10}$ and slope of m = 3.0 (Wöhler exponent), selected from the recommended values in DNV (2021) for studless chain mooring in corrosive environment. After estimating $DEL_{Lifetime}$, one can define the fatigue limit state for the mooring lines as below in Equation 6:

$$g_{Fatigue}(X) = \Delta - \frac{n_{eq}DEL_{Lifetime}^{m}}{Q}$$
 (6)

where Δ is the fatigue damage limit for the material. In this work, the limit state is considered deterministic, and hence Δ is taken as 1.

Input features for the surrogate model Variable Distribution U Weibull U_{dir} von Mises σ_u Log Normal H_s Weibull W_{dir} von Mises T_p Log Normal R_f Uniform D_{buoy} Uniform

Output features for the surrogate model Limit State Quantity of Interest Unit Surge mPitch Tower Top Acceleration fa $[N/s^2]$ Tower Top Acceleration ss $[N/s^2]$ Pontoon Bending kNMooring Line DEL Mpa

A sensitivity analysis is conducted by considering six different cases for different seed configurations and four different simulation lengths to identify the required simulation length and number of seeds for a feasible DOE. Considered cases The cases considered are presented in Table 8. Generally, 10-minute simulations are enough for representing turbulence characteristics, and it is important to separate mean wind conditions from turbulent fluctuations (Burton et al., 2011), but a longer simulation length is vital to capture low-frequency dynamics/loads on the floating structure, which is essential for the floating wind turbines (due to lower surge natural frequencies, especially). For this sensitivity analysis, only a 12 m/s wind speed is considered, and the environmental conditions are selected from the distribution defined in Equation 3. As a measure of control, the median values of each simulation are used, and the percent root mean square (RMS) error is calculated based on six wind and three

wave seeds. Considering the findings from this part, it is decided to use three wind seeds and two wave seeds with a 1400 s simulation length, including a 200 s transient period. The results are presented in Figue 5. This analysis is case dependent, and one should consult the relevant design guidelines such as (DNV, 2014; Veritas, 2010; iec, 2019).

Table 8. Cases considered for the wind seed, wave seed, and simulation length.

Case	Wind Seed	Wave Seed	Simulation Length [s]
Case 1	3	1	800, 1400, 2000, 3800
Case 2	3	2	800, 1400, 2000, 3800
Case 3	4	2	800, 1400, 2000, 3800
Case 4	4	3	800, 1400, 2000, 3800
Case 5	5	3	800, 1400, 2000, 3800
Case 6	6	3	800, 1400, 2000, 3800

Only a 12 m/s wind speed is considered for the sensitivity analysis, and the environmental conditions are selected from the distribution defined in Equation 3. As a measure of variability, the percent error is calculated based on the median value of six wind and three wave seeds for each time series. Our reference for the error comparison is the case with the highest number of seeds (Six wind and three wave realizations) for each simulation length. The results of this sensitivity analysis are presented for three quantities of interest, including the mooring line tension, tower base moment, and the thrust force.

The results of the sensitivity study are presented in Figure 5. The reader should interpret these results in light of the tradeoff between computational cost and accuracy. Statistically, using more realizations can increase the accuracy of postprocessing; however, we may also lose information on the floater's low-frequency response if the simulation length is not sufficiently long. So, using the results in Figure 5, the readers can select the tradeoff between different numbers of wind and wave realizations for obtaining sufficiently accurate statistics for a selected simulation length. This analysis is case dependent, and one should consult the relevant design guidelines such as (DNV, 2014; Veritas, 2010; iec, 2019). Considering the findings from the sensitivity study, we decided to use three wind seeds and two wave seeds with a 1400-second simulation length, including a 200-second transient period. We built our deterministic surrogate model based on the median of outputs from random seeds for each environmental case.

3.5.2 Implementing the Surrogate Model

435

Surrogate model parameters (i.e., hyperparameters) should be tuned for the specific dataset, and there are several available methods for hyperparameter optimization. In this work, we opted to use Bayesian optimization. Bayesian optimization requires fewer iterations and converges to better optimal solutions in less time than traditional hyperparameter tuning algorithms, such as grid search and random search (Snoek et al., 2012). For the surrogate model fitting, we split the input dataset into test and training sets (20 % test and 80 % training), and used the test dataset to validate the model. The FNN architecture consists of two hidden layers with Rectified Linear Unit (RELU) activation functions, and one output layer with a single neuron with a linear activation function as required for regression tasks. Due to efficient gradient propagation, improved computational costs,

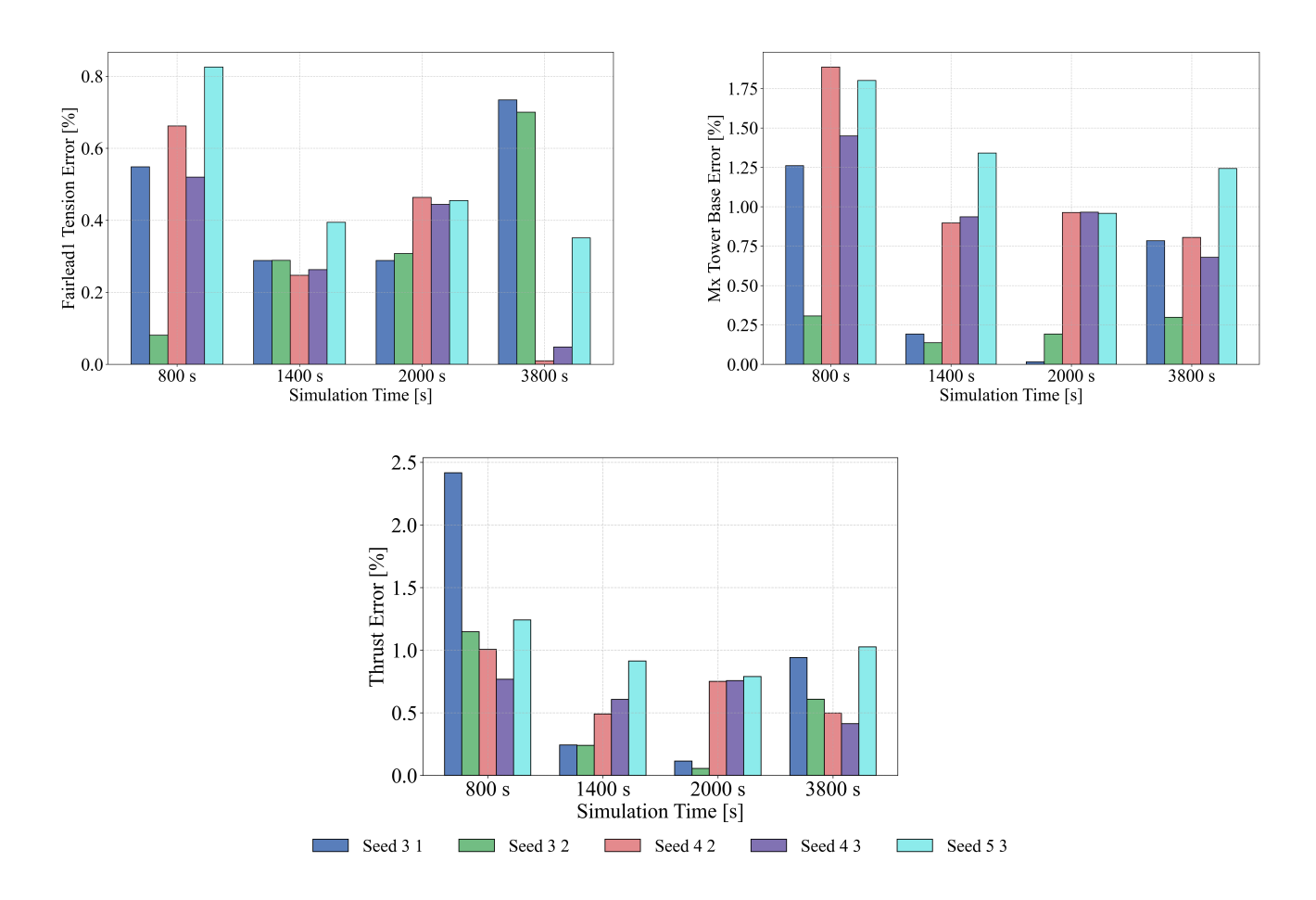


Figure 5. Percent Absolute Error absolute error for Different Number different number of Seeds wave and wind seeds with respect to simulation length

and good convergence properties (Alba et al., 2021), the RELU activation is preferred. The model accuracy is validated using different error metrics, including RMSE and the coefficient of determination (R-squared value).

3.6 Second Step: Optimization Based on Global Structural Response Computed in Time Domain

Global system performance is preferred when investigating different floater characteristics and evaluating the limit states. The global limit states considered in this study are divided into three main types: ultimate limit state (ULS), fatigue limit state (FLS), and serviceability limit state (SLS). SLS is defined We defined SLS as the maximum allowable floater offset that avoids to avoid dynamic cable damage; FOWT pitch angle, which determines system stability and power generation; and, FWT pitch angle to determine system stability, and limit power loss. Finally, the nacelle acceleration limit, which prevents damage to the drivetrain and preserves its fatigue life set for a safe operation of the turbine. ULS is defined as a maximum mooring line

tensile load, floater pontoon buckling, and tower base bucklingand floater pontoon bending. FLS is defined in terms of the lifetime fatigue of the structure's mooring lines. The design optimization in the time domain is conducted for multiple limit states simultaneously, while separate surrogate models are trained for each limit state based on the same training dataset. In Table 9, the global limit states for the second stage of the optimization are presented. SLS are given as $g_{11}(x_1)$ for dynamic surge motion, $g_{12}(X)$ for the dynamic pitch angle, $g_{13}(X)$ is for the maximum nacelle acceleration. $g_{14}(X)$ static pontoon bending $g_{15}(X)$ and maximum mooring line tension $g_{16}(X)$ are ULS and mooring line fatigue lifetime fatigue for mooring line 1 and mooring line 2 defined as $g_{16}(X)$ and $g_{17}(X)$.

Table 9. Design Constraints for the first part of the optimization where δ_1 is the surge motion, δ_2 is the dynamic pitch angle, $a_{nacelle}$ is the tower top acceleration, and T_{max} is the maximum mooring line tension predicted by the surrogate model. T_{cr} is the mooring line tension capacity and σ_{design} is the bending load on the pontoons. $D_{Life,moor1}$ and $D_{Life,moor2}$ are the lifetime fatigue capacities of the mooring lines.

Constraint	Description		Unit		
	Serviceability Limit States				
$g_{11}(X)$	Dynamic Surge offset	$\delta_1 - 40$	m		
$g_{12}(X)$	Dynamic Pitch angle	$\delta_2 - 10$ (Dou et al., 2020; Leimeister et al., 2020b)	0		
$g_{13}(X)$	Nacelle acceleration side side (ss)	$a_{nacelle} - 1.962$ (Leimeister et al., 2020b)	m/s ²		
$g_{14}(X)$	Nacelle acceleration fore aft (fa)	$a_{nacelle} - 1.962$ (Leimeister et al., 2020b)	$\underset{\sim}{\text{m/s}^2}$		
	Ultimate Limit States				
$g_{14}(X)$ $g_{15}(X)$	Mooring line 1 tension	$T_{max} - T_{cr}$	kN		
$g_{15}(X)$ $g_{16}(X)$	Static pontoon bending	$\sigma_{design} - \sigma_{cr}$	MPa kN €		
Fatigue Limit States					
$g_{16}(X)$ $g_{17}(X)$	Lifetime fatigue for mooring line 1	$D_{Life,moor1} - 1$	-		
$g_{17}(X) g_{18}(X)$	Lifetime fatigue for mooring line 2	$D_{Life,moor2} - 1$	-		

The dynamic optimization constraints are selected based on the system dynamics and production limits, considering the practices seen in literature. Dynamic surge motion is restricted, considering the maximum dynamic floater offset determined by the designer and the mooring line design characteristics. In literature, there are various ways of selecting this value. Pollini et al. (2023) used 25 % of the water depth as dynamic surge displacement criteria, where (Leimeister et al., 2020b) used 20 % of the water depth as the static surge displacement criteria and then minimized the dynamic surge motion within the optimization. A strict nacelle acceleration constraint is implemented for operational reasons to avoid lubrication problems for the sensitive nacelle components (Leimeister et al., 2020b). Constraints for the ULS are defined based on the tension failure of the mooring lines and tower base yielding, which are critical for the integrity of the FWT assets. The final limit states (FLS) considered are those related to the fatigue lifetime of the mooring lines, which is critical for the stability and station-keeping of the entire system, as well as preventing fatigue failure during the FWT lifetime.

4 Results

495

500

505

510

4.1 Low Cost Design Evaluation: First Step

This section presents the results of the analytical design constraint evaluation. The boundaries for each design constraint considered can be seen. The initial step of our approach is to reduce the design space by evaluating the analytical design constraints. As discussed in Section 3.1, these include natural frequencies, stability, and static pitch angle under rated wind speed. The results are presented in Figure 6-, where subfigures 6a to 6f present the order of constraint evaluation. In Figure 6, the samples shown are infeasible designs, and different colors indicate the active constraints that render the designs infeasible.

In Figure 6a, surge natural frequency constraint (g₁(X)) eliminates the designs at the lower left corner of the DOE. Pitch natural frequency lower (g₂(X)) and upper (g₃(X)) constraints narrows the feasible design space further. Evaluating tower natural frequency (g₄(X)) and system stability (g₅(X)) constraints causes fewer infeasible design points compared to pitch natural frequency and static pitch angle (g₆(X)) constraints. When all analytical design constraints are considered as in Figure 6f, the final feasible design space is bounded by the static pitch angle and pitch natural frequency constraint. This result is concept and design variable-dependent, and different shapes can be obtained with different variables.

Surge natural frequency constraint Pitch natural frequency constraint (low)

Pitch natural frequency constraint (high) Tower natural frequency constraint

Stability Constraint Static Pitch Angle

Analytical design constraints evaluated sequentially for the initial DOE screening After running the analytical design constraint evaluation, the Pareto fronts of the feasible design space are defined to identify its boundaries. The exact boundary fit is offset to include potentially feasible design points that may not be captured by the relatively crude sampling used in the first optimization stage. We observe that in the present case the Pareto fronts can be approximated by a power law. The boundaries of a design space parameterized with a power law decay function can be seen in Figure 7a, and the resulting DOE for the time domain evaluation can be seen in Figure 7b —with LCOE values. The LCOE values have a decreasing trend towards longer floater radius and smaller outer column diameter.

4.2 Time Domain Design Evaluation: Second Step

The second phase of the optimization includes results from the global limit states. Figure 8 presents the reference design and optimized design geometries side-by-side, and Figure 9 presents the iteration history of the design variables and objective function. Compared to the baseline design, floater radius x_1 has an increasing trend with the number of evaluations, and the outer column diameter x_2 decreases. Considering our objective function LCOE, this results in a lower objective function value. As shown in Figure 10, the design driving constraints are mooring line fatigue active constraints are the mooring line 1 fatigue $(g_{17}(X))$, which is in the direction of loading, and the lower boundary from the first step of the design optimization. Design constraints, such as mooring 2 fatigue $(g_{18}(X))$, mooring 1 tension $(g_{15}(X))$, and tower top accelerations, do not affect our optimal solution. During the initial optimization iterations, the dynamic pitch angle constraint $(g_{12}(X))$ was active, and it became inactive with increasing floater radius and decreasing outer column diameter. As presented in Figure 6, the lower

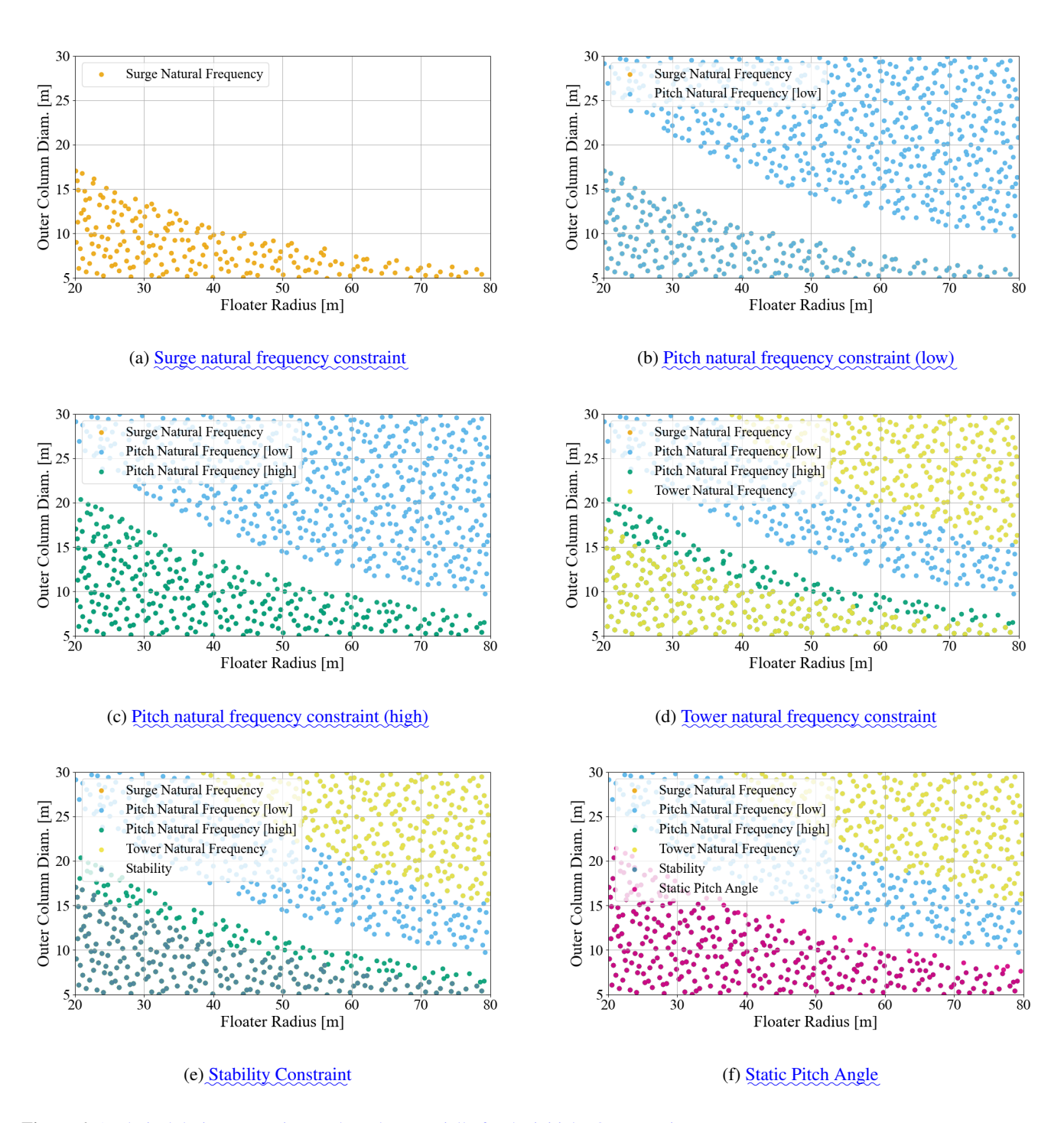
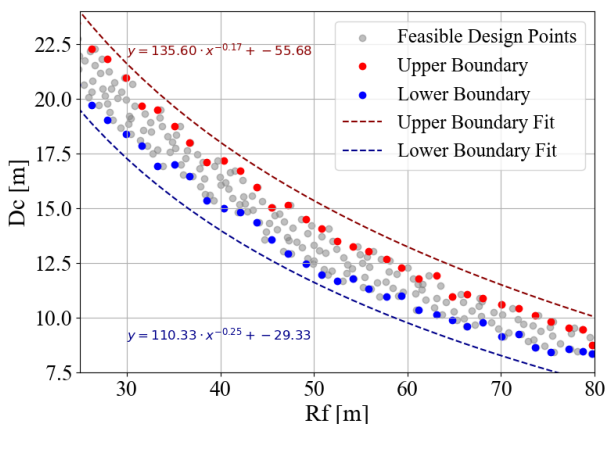
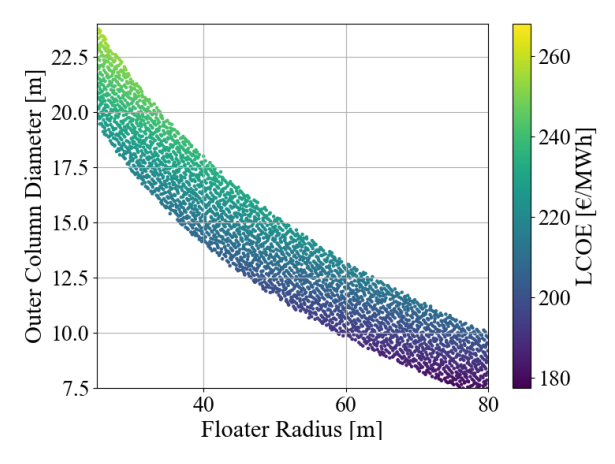


Figure 6. Analytical design constraints evaluated sequentially for the initial DOE screening

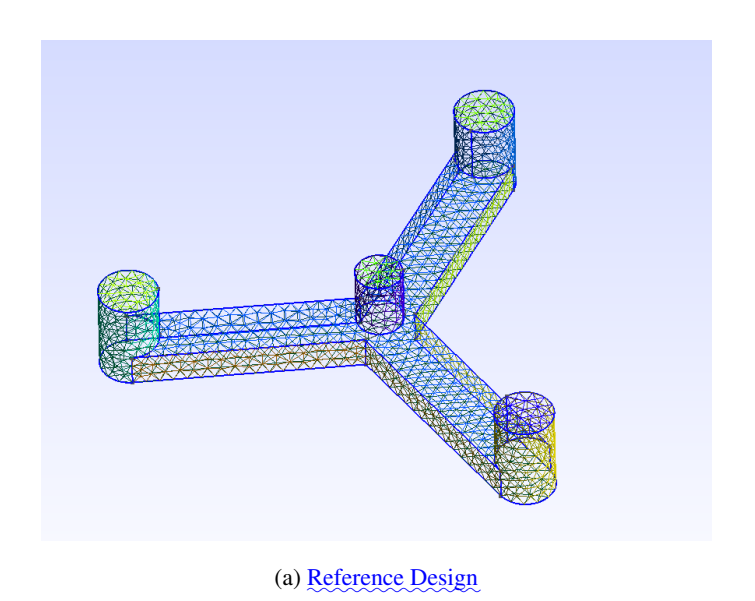


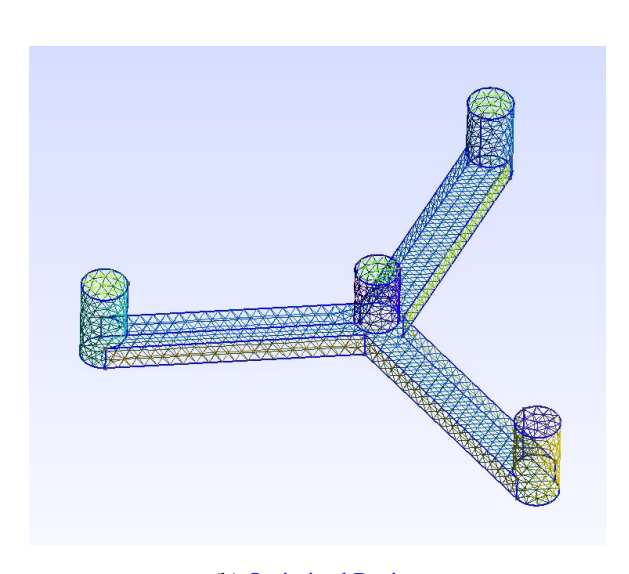


(a) Boundary fit to the feasible design space (b) Latin hypercube grid of the feasible design space

Figure 7. Refined design space after the analytical limit state evaluation

boundary defining our feasible design space is determined by the mean pitch angle at rated wind speed. Mooring line design has effects on both active constraints. By changing the mooring line parameters, one may further improve the design, where co-design approaches might be implemented.





(b) Optimized Design

Figure 8. Comparison of reference and optimized design

The resulting design has 60.18 m floater radius and 10.3 m buoyancy outer column diameter with LCOE of 176.9 €/MWh, which is a 3.7 % decrease from the nominal value. Key load responses of the optimized design are also compared to the baseline

design as presented in Figure 12. The simulations for this comparison are performed using HAWC2 (Bischoff Kristiansen, 2022), and the same wind and wave seeds are used to eliminate seed uncertainty. Median time series statistics are used for the 2000s simulations. The simulations are performed for the operational range with NTM turbulence. Figure 12 presents that, regarding aerodynamics, both designs have the same responses for the generated power and blade root moment. There are no visible differences for the hydrodynamic loads/responses. The difference is higher for the above-rated region for the mooring line tension. As it is presented in Figure 11, pitch response is higher compared to the reference design. The response is still within the allowable limit of 10 degrees. Considering those findings, we can say that both designs show similar behavior, but for further design verification, additional simulations and potentially higher-fidelity analysis should be performed. Reference and optimized designs are also compared considering the AEPs for the South Brittany Site. The AEP of the reference design is calculated as 85.93 GWh and the AEP of the optimized design is estimated at 85.74 GWh which is 0.2211 % lower than the reference design. The difference is mainly due to the larger pitch response of the optimized floater where this tradeoff should be considered as well.

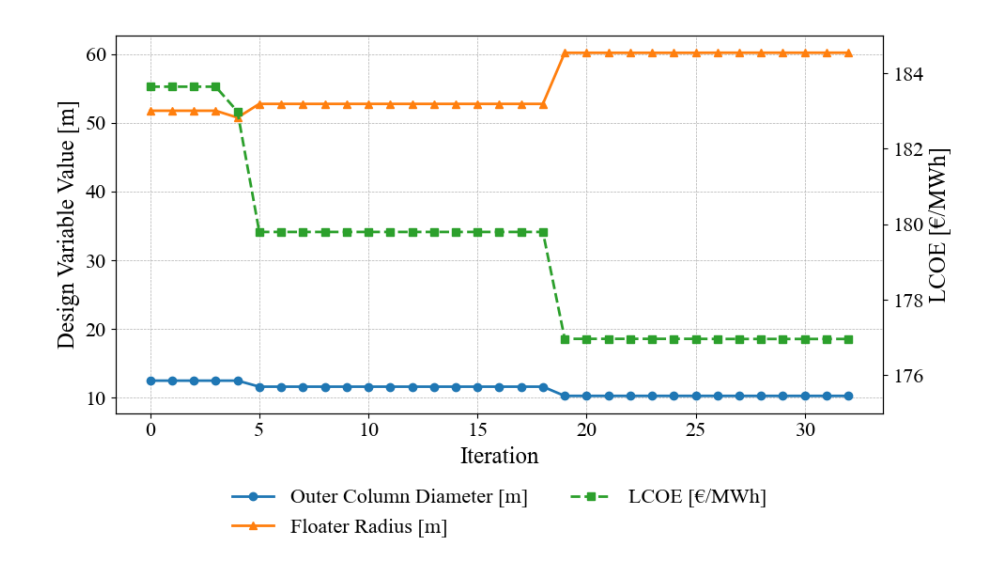


Figure 9. Design variables and cost values during the iteration for the optimization with mooring line FLS

5 Discussion

525

The method presented in this paper has several advantages, including the effective combination of analytical constraints and surrogate modeling to reduce computational complexity. It—With our approach, we obtained a significant decrease in the computational cost of the optimization problem. This is achieved by two important steps: replacing time-domain load simulations with a surrogate model and reducing DOE for surrogate training. Using a surrogate model within the optimization

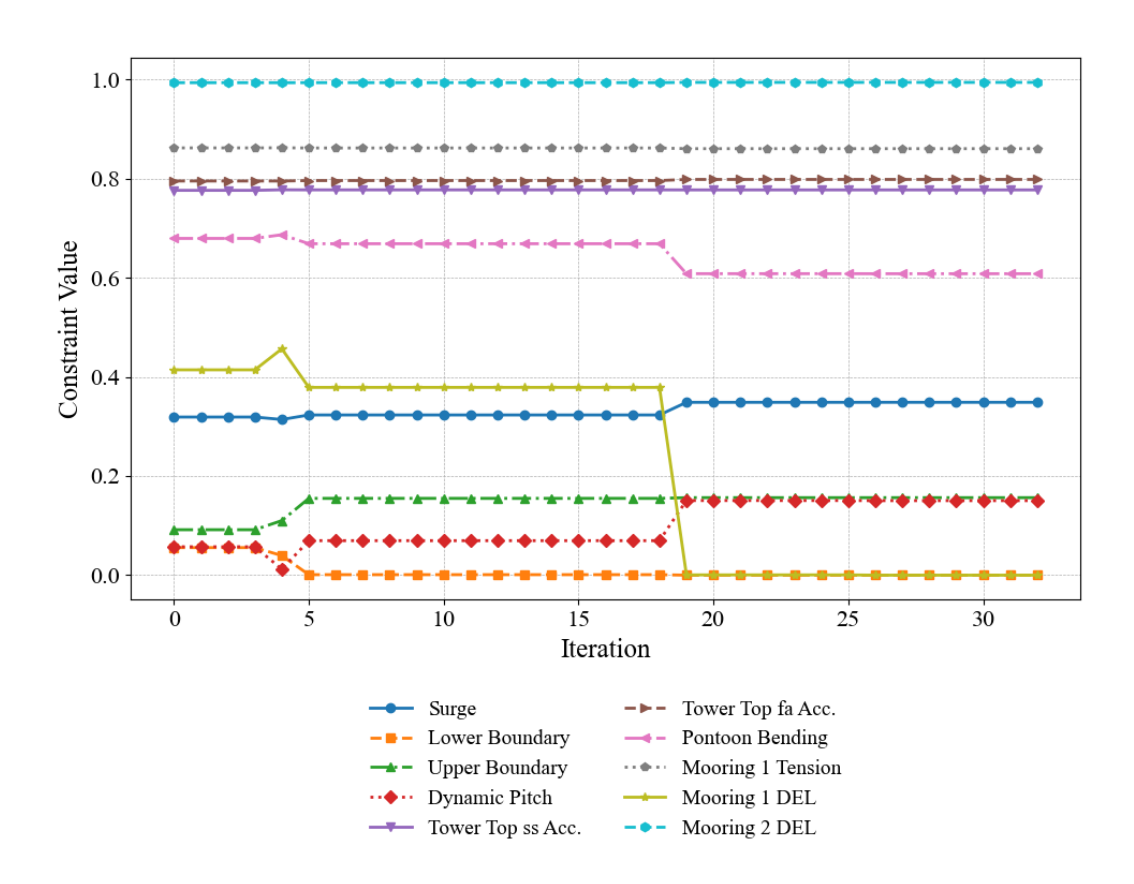


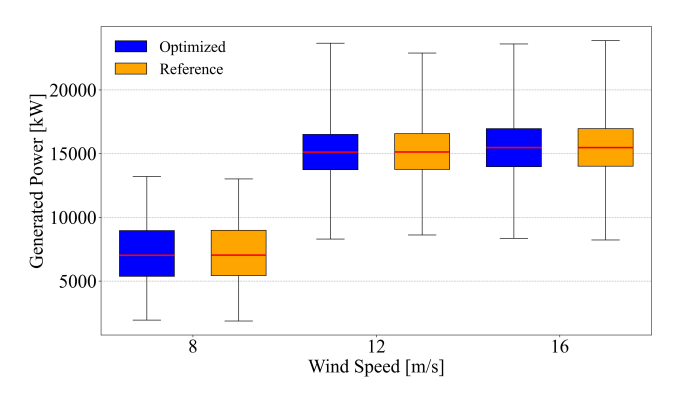
Figure 10. Reference DesignConstraint values for the iteration with mooring line FLS

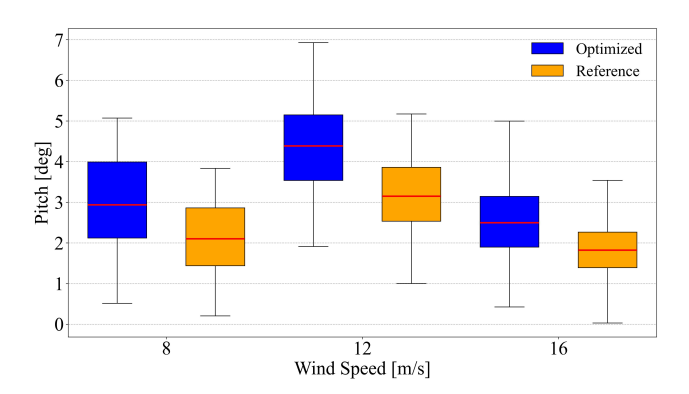
Optimized Design Comparison of reference and optimized design

535

process results in a reduction of 98.72 % of simulations to run. Without a surrogate model, about 1.6 million ten-minute simulations should be performed for the optimization process. With our approach, only 20400 aeroelastic simulations should be performed for surrogate model training. A second improvement is due to reducing the DOE area for surrogate model training, whereby, focusing only on the feasible design space, the sampling space for surrogate training is decreased by 89.4 %. Therefore, our approach enables the evaluation of limit states based on high-fidelity time-domain analyses without excessive computational costs. Due to the flexibility of the framework, additional design variables or limit states can be added, which offers a practical balance between conceptual simplicity and detailed accuracy, ideal for iterative optimization processes.

The presented algorithm also faces limitations and challenges. A significant part of the computational cost associated with the use of the framework is due to the data generation required for surrogate model training. HPC simulations are currently the only feasible approach for generating the surrogate training set. In the present study, the simulations were performed on the Sophia HPC cluster owned by the Technical University of Denmark. Depending on the complexity of the aeroleastic model, this phase can be improved further. The computational cost for surrogate model training and for optimization (both the first step





(a) Iteration history—Comparison of power generation for the optimized and baseline design variables

550

555

560

565

(b) <u>Iteration history Comparison</u> of the objective function pitch response for optimized and baseline design

Figure 11. Design variables Comparison of power generation properties of optimized and eost values during the iteration for the optimization with mooring line FLS baseline design.

and the second step as described earlier) is in the order of minutes on a single CPU, which is negligible compared to the training data generation cost. For increasing accuracy of the surrogate model, different sampling techniques can be implemented, the DOE of the surrogate can be enriched incrementally using active learning approach, and additional environmental conditions can be considered.

The cost of generating surrogate model training data has to be weighted weighted against considerations on the accuracy of the resulting surrogate, as well as the representativeness of the design problem. Considering a limited number of design variables can cause neglect of additional influential design variables, such as structural thickness and mooring design properties.

The steel plate thickness is considered constant throughout the floater, which is likely not representative of the final floater design. This should be further investigated in the detailed design phase using FEM (Finite Element Modeling).

The bending limit state is considered only for the static loading case. To indirectly include dynamic effects, an adjustment factor can be implemented within the optimization problem. Within our approach, we developed an algorithm that is suitable for uncertainty propagation within the design optimization process. Currently, we have only considered the environmental uncertainties by sampling from the environmental distributions of the selected site. In an addition to our approach, one can consider the effects of other uncertainties, such as material, load, and model, within the optimization.

Finally, the results obtained from this work demonstrated the potential of surrogate-based optimization methods for meaningful LCOE reduction in FWT designs. They also highlighted the feasibility and accuracy in bridging the gap between conceptual and detailed designs, which indicates significant potential for broader application across different FWT concepts and larger-scale optimization problems. Future work should aim to expand the optimization scope to include more detailed design variables, incorporate robust or reliability-based design optimization to address uncertainties, and evaluate a wider range of optimization algorithms. Additionally, exploring probabilistic surrogate models could enhance the ability to quantify and manage uncertainties inherent in offshore wind conditions and cost estimations.

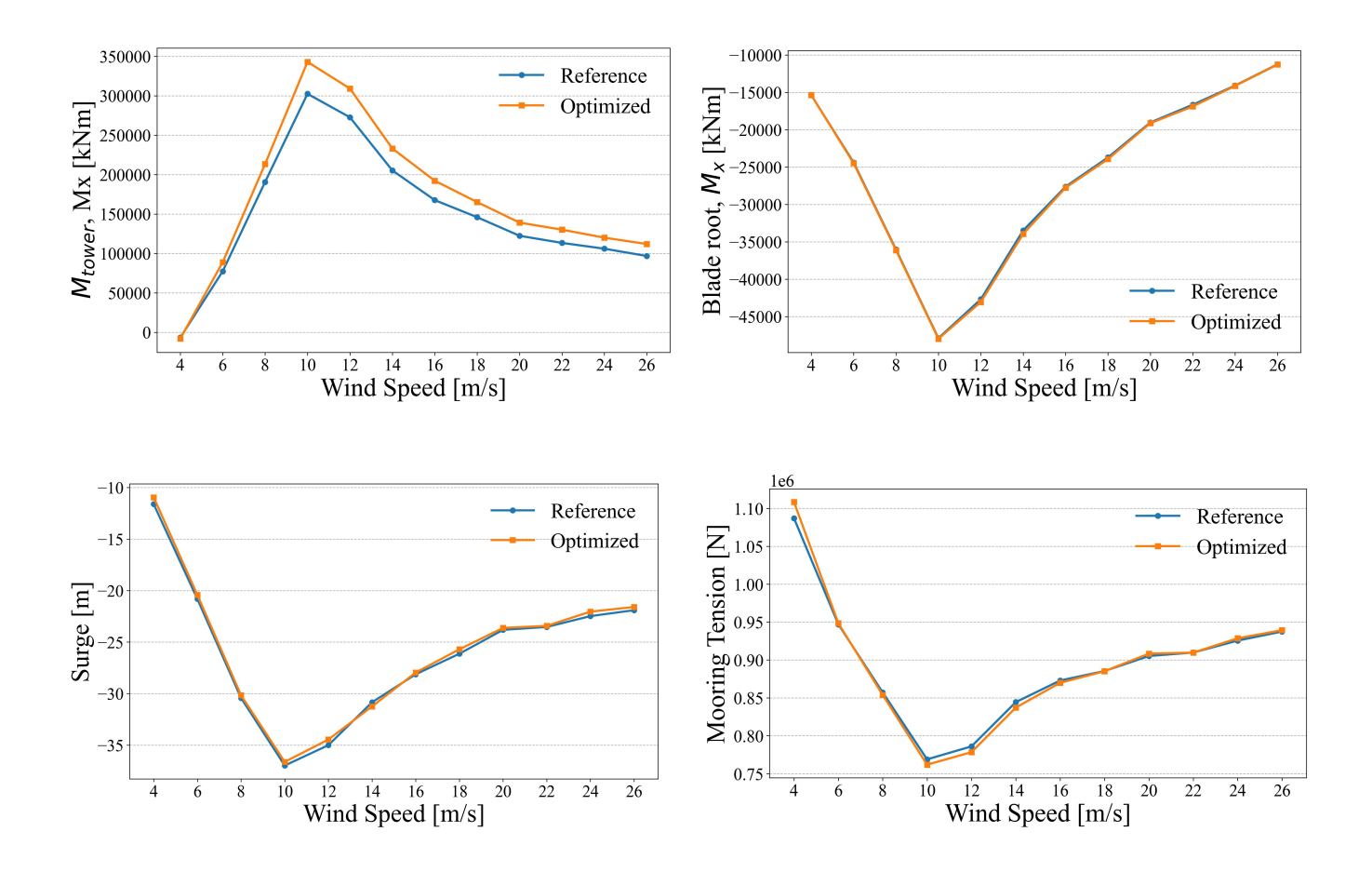


Figure 12. Constraint values Median key load response comparison for the iteration optimized design with mooring line FLSthe reference case using HAWC2 simulations.

6 Conclusion

570

This study demonstrated a two-step surrogate-based optimization framework suitable to the design of floating wind turbine (FWT) substructures. The approach effectively implements analytical constraints to initially narrow down the feasible design space, and then applying surrogate models trained with high-fidelity time-domain simulations for detailed design evaluation against fatigue, serviceability, and ultimate limit states. By optimizing the buoyancy outer column diameter and floater radius of a UMaine semisubmersible platform coupled with the IEA 15 MW turbine, the proposed methodology achieved a meaningful reduction of 3.7 % in the Levelized Cost of Energy (LCOE)LCOE, ensuring that all global structural limit states—including ultimate, fatigue, and serviceability—, were met.

The novelty of this work lies in the integration of analytical constraints and surrogate modeling within a deterministic design optimization procedure, enabling accurate, computationally efficient exploration of complex design spaces. This bridges the

gap between conceptual simplicity and detailed accuracy, offering a practical optimization tool suitable for real-world FWT design scenarios. Practically, the resulting framework not only facilitates significant economic improvements by reducing LCOE but also enhances design reliability, contributing directly to the advancement of floating offshore wind technology.

Future studies should expand this optimization framework by incorporating additional influential design variables, such as structural thickness, ballast configuration, and mooring system properties. Further research could integrate probabilistic surrogate models or robust/reliability-based design optimization methods to explicitly address the inherent uncertainties of offshore wind environments. Lastly, evaluating alternative optimization algorithms and extending validation to other FWT concepts would enhance the robustness and applicability of this optimization approach across broader engineering contexts.

Author contributions. BY: Conceptualization, methodology, investigation, writing (original draft), software, and visualization. ND: Conceptualization, methodology, writing (review and editing), and supervision. AK: Supervision, writing (review and editing). ABA: Supervision, methodology, writing (review and editing).

Competing interests. The authors declare that one or more authors are members of the editorial board of WES journal.

580

Acknowledgements. The authors gratefully acknowledge the computational and data resources provided on the Sophia HPC Cluster at the Technical University of Denmark, DOI: 10.57940/FAFC-6M81. This work is funded by the Department of Wind and Energy Systems at the Technical University of Denmark. The support is greatly appreciated.

References

- A Direct Search Optimization Method That Models the Objective and Constraint Functions by Linear Interpolation, in: Advances in Optimization and Numerical Analysis, pp. 51–67, Springer Netherlands, Dordrecht, ISBN 978-90-481-4358-0 978-94-015-8330-5, https://doi.org/10.1007/978-94-015-8330-5 4, 1994.
- Modelling techniques for optimizing metal forming processes, in: Microstructure Evolution in Metal Forming Processes, pp. 35–66, Elsevier, ISBN 978-0-85709-074-4, https://doi.org/10.1533/9780857096340.1.35, 2012.
 - IEC 61400-1: Wind energy generation systems Part 1: Design requirements, Technical Report, International Electrotechnical Commission, Geneva, Switzerland, 2019.
 - Agency, D. E.: Generation of Electricity and District heating, Tech. Rep. 0015, Danish Energy Agency, Copenhagen, Denmark, 2016.
- Alba, E., Luque, G., Chicano, F., Cotta, C., Camacho, D., Ojeda-Aciego, M., Montes, S., Troncoso, A., Riquelme, J., and Gil-Merino, R., eds.: Advances in Artificial Intelligence: 19th Conference of the Spanish Association for Artificial Intelligence, CAEPIA 2020/2021, Málaga, Spain, September 22–24, 2021, Proceedings, Lecture Notes in Computer Science, Springer International Publishing, Cham, ISBN 978-3-030-85712-7 978-3-030-85713-4, https://doi.org/10.1007/978-3-030-85713-4, iSSN: 0302-9743, 1611-3349, 2021.
- Allen, C., Viscelli, A., Dagher, H., Goupee, A., Gaertner, E., Abbas, N., Hall, M., and Barter, G.: Definition of the UMaine VolturnUS-S

 Reference Platform Developed for the IEA Wind 15-Megawatt Offshore Reference Wind Turbine, Tech. Rep. NREL/TP–5000-76773, 1660012, MainId:9434, https://doi.org/10.2172/1660012, 2020.
 - Backwell, B., Lee, J., Patel, A., Qiao, L., Nguyen, T., Liang, W., Fang, E., Cheong, J., Tan, W. H., Francisco, A. M., Bui, T. V., Nguyen, T., Fiestas, R., Cox, R., de Lima, J. P., Rabie, H., Ladwa, R., Madan, K., Muchiri, W., Weekes, N., Khinda, N., and Yamamura, J.: GWEC Global Offshore Wind Report, 2024.
- Baudino Bessone, M., Singh, D., Kalimeris, T., Bachynski-Polić, E., and Viré, A.: Surrogate-assisted optimization of floating wind turbine substructure, Journal of Physics: Conference Series, 2767, 062 032, https://doi.org/10.1088/1742-6596/2767/6/062032, 2024.
 - Biran, A. and López-Pulido, R.: Ship hydrostatics and stability, Elsevier: Butterworth-Heinemann, Amsterdam, second edition edn., ISBN 978-0-08-098287-8, 2014.
 - Bischoff Kristiansen, M.: Welcome to HAWC2, https://www.hawc2.dk/hawc2-info, 2022.
- Borg, M. and Bredmose, H.: D4.4 Overview of the numerical models used in the consortium and their qualification, 2015.
 - Borg, M. and Collu, M.: Offshore floating vertical axis wind turbines, dynamics modelling state of the art. Part III: Hydrodynamics and coupled modelling approaches, Renewable and Sustainable Energy Reviews, 46, 296–310, https://doi.org/10.1016/j.rser.2014.10.100, 2015.
- Borisade, F., Gruber, J., Hagemann, L., Kretschmer, M., Lemmer, F., Müller, K., Schliph, D., Nguyen, N.-D., and Vita, L.: D 7.4 State-ofthe-Art FOWT design practice and guidelines, Unrestricted, University of Stuttgart, Stuttgart, 2016.
 - Burton, T., Jenkins, N., Sharpe, D., and Bossanyi, E.: Wind Energy Handbook, Wiley, 1 edn., ISBN 978-0-470-69975-1 978-1-119-99271-4, https://doi.org/10.1002/9781119992714, 2011.
 - Capaldo, M., Guiton, M., Huwart, G., Julan, E., Dimitrov, N. K., Kim, T., Lovera, A., and Peyrard, C.: Design brief of HIPERWIND offshore wind turbine cases: bottom fixed 10MW and floating 15MW, 2021a.
- 625 Capaldo, M., Julan, E., Lovera, A., and Peyrard, C.: Hiperwind D1.2: Design brief for the use cases and models in engineering tools, Confidential, 2021b.

- Cousin, A., Garnier, J., Guiton, M., and Munoz Zuniga, M.: A two-step procedure for time-dependent reliability-based design optimization involving piece-wise stationary Gaussian processes, Structural and Multidisciplinary Optimization, 65, https://doi.org/10.1007/s00158-022-03212-1, publisher: Springer Science and Business Media LLC, 2022.
- Dimitrov, N. and Natarajan, A.: Wind farm set point optimization with surrogate models for load and power output targets, Journal of Physics: Conference Series, 2018, 012 013, https://doi.org/10.1088/1742-6596/2018/1/012013, 2021.
 - DNV: DNV-OS-E301 Position Mooring, 2021.
 - DNV, G. L.: DNV-OS-J101-Design of offshore wind turbine structures., 2014.
- Dou, S., Pegalajar-Jurado, A., Wang, S., Bredmose, H., and Stolpe, M.: Optimization of floating wind turbine support structures using frequency-domain analysis and analytical gradients, Journal of Physics: Conference Series, 1618, 042 028, https://doi.org/10.1088/1742-6596/1618/4/042028, 2020.
 - Esteban, M. D., Diez, J. J., López, J. S., and Negro, V.: Why offshore wind energy?, Renewable Energy, 36, 444–450, https://doi.org/10.1016/j.renene.2010.07.009, 2011.
 - Europe, W.: Floating Offshore Wind Vision Statement, 2017.
- 640 Forum, O. E.: Ocean Energy Strategic Roadmap Building Ocean Energy for Europe, 2016.
 - Gaertner, E.: Definition of the IEA wind 15-megawatt offshore reference wind turbine, Tech. Rep. TP-5000-75698, NREL, Golden, CO, 2020.
 - Geuzaine, C. and Remacle, J.-F.: Gmsh: a three-dimensional Finite element mesh generator with built-in pre- and post-processing facilities, International Journal for Numerical Methods in Engineering, 2009.
- 645 GL, D.: DNVGL-ST-0119: Floating wind turbine structures, Tech. rep., 2018.
 - Hegseth, J. M., Bachynski, E. E., and Martins, J. R.: Integrated design optimization of spar floating wind turbines, Marine Structures, 72, 102 771, https://doi.org/10.1016/j.marstruc.2020.102771, 2020.
 - Hegseth, J. M., Bachynski, E. E., and Leira, B. J.: Effect of environmental modelling and inspection strategy on the optimal design of floating wind turbines, Reliability Engineering & System Safety, 214, 107 706, https://doi.org/10.1016/j.ress.2021.107706, 2021.
- 650 Jiang, Z.: Installation of offshore wind turbines: A technical review, Renewable and Sustainable Energy Reviews, 139, 110576, https://doi.org/10.1016/j.rser.2020.110576, 2021.
 - Journée, J. M. J. and Massie, W. W.: Offshore Hydromechanics, 2001.
 - Karimi, M., Hall, M., Buckham, B., and Crawford, C.: A multi-objective design optimization approach for floating offshore wind turbine support structures, Journal of Ocean Engineering and Marine Energy, 3, 69–87, https://doi.org/10.1007/s40722-016-0072-4, 2017.
- 655 Kennedy', J. and Eberhart, R.: Particle Swarm Optimization, 1995.
 - Leimeister, M. and Kolios, A.: Reliability-based design optimization of a spar-type floating offshore wind turbine support structure, Reliability Engineering & System Safety, 213, 107 666, https://doi.org/10.1016/j.ress.2021.107666, publisher: Elsevier BV, 2021.
 - Leimeister, M., Kolios, A., and Collu, M.: Development and Verification of an Aero-Hydro-Servo-Elastic Coupled Model of Dynamics for FOWT, Based on the MoWiT Library, Energies, 13, 1974, https://doi.org/10.3390/en13081974, 2020a.
- Leimeister, M., Kolios, A., Collu, M., and Thomas, P.: Design optimization of the OC3 phase IV floating spar-buoy, based on global limit states, Ocean Engineering, 202, 107 186, https://doi.org/10.1016/j.oceaneng.2020.107186, 2020b.
 - Lerch, M., De-Prada-Gil, M., Molins, C., and Benveniste, G.: Sensitivity analysis on the levelized cost of energy for floating offshore wind farms, Sustainable Energy Technologies and Assessments, 30, 77–90, https://doi.org/10.1016/j.seta.2018.09.005, 2018.

- Liu, Y.: HAMS: A Frequency-Domain Preprocessor for Wave-Structure Interactions—Theory, Development, and Application, Journal of Marine Science and Engineering, 7, 81, https://doi.org/10.3390/jmse7030081, 2019.
 - Matha, D., Sandner, F., Molins, C., Campos, A., and Cheng, P. W.: Efficient preliminary floating offshore wind turbine design and testing methodologies and application to a concrete spar design, Philosophical Transactions of the Royal Society A: Mathematical, Physical and Engineering Sciences, 373, 20140 350, https://doi.org/10.1098/rsta.2014.0350, 2015.
- Meng, F., Lio, W. H., Pegalajar-Jurado, A., Pierella, F., Hofschulte, E. N., Santaya, A. G., and Bredmose, H.: Experimental study of floating wind turbine control on a TetraSub floater with tower velocity feedback gain, Renewable Energy, 205, 509–524, https://doi.org/10.1016/j.renene.2023.01.073, 2023.
 - Muskulus, M. and Schafhirt, S.: Design Optimization of Wind Turbine Support Structures—A Review, Journal of Ocean and Wind Energy, 1, 2014.
- Myhr, A., Bjerkseter, C., Ågotnes, A., and Nygaard, T. A.: Levelised cost of energy for offshore floating wind turbines in a life cycle perspective, Renewable Energy, 66, 714–728, https://doi.org/10.1016/j.renene.2014.01.017, 2014.
 - Ojo, A., Collu, M., and Coraddu, A.: A Review of Design, Analysis and Optimization Methodologies for Floating Offshore Wind Turbine Substructures, SSRN Electronic Journal, https://doi.org/10.2139/ssrn.3936386, 2021.
 - Ojo, A., Collu, M., and Coraddu, A.: Multidisciplinary design analysis and optimization of floating offshore wind turbine substructures: A review, Ocean Engineering, 266, 112 727, https://doi.org/10.1016/j.oceaneng.2022.112727, 2022.
- Patryniak, K., Collu, M., and Coraddu, A.: Multidisciplinary design analysis and optimisation frameworks for floating offshore wind turbines: State of the art, Ocean Engineering, 251, 111 002, https://doi.org/10.1016/j.oceaneng.2022.111002, 2022.
 - Pegalajar-Jurado, A., Borg, M., and Bredmose, H.: An efficient frequency-domain model for quick load analysis of floating offshore wind turbines, Wind Energy Science, 3, 693–712, https://doi.org/10.5194/wes-3-693-2018, 2018.
- Pillai, A. C., Thies, P. R., and Johanning, L.: Comparing Frequency and Time Domain Simulations for Geometry Optimization of a Floating
 Offshore Wind Turbine Mooring System, in: ASME 2018 1st International Offshore Wind Technical Conference, p. V001T01A016, American Society of Mechanical Engineers, San Francisco, California, USA, ISBN 978-0-7918-5197-5, https://doi.org/10.1115/IOWTC2018-1006, 2018.
 - Pollini, N., Pegalajar-Jurado, A., and Bredmose, H.: Design optimization of a TetraSpar-type floater and tower for the IEA Wind 15 MW reference wind turbine, Marine Structures, 90, 103 437, https://doi.org/10.1016/j.marstruc.2023.103437, 2023.
- Ragonneau, T. M.: Model-Based Derivative-Free Optimization Methods and Software, Ph.D. thesis, Hong Kong Polytechnic University, https://arxiv.org/abs/2210.12018, version Number: 5, 2022.
 - Rosenblatt, M.: Remarks on a Multivariate Transformation, The annals of mathematical statistics, 23, 470-472, 1952.
 - Schröder, L., Krasimirov Dimitrov, N., Verelst, D. R., and Sørensen, J. A.: Wind turbine site-specific load estimation using artificial neural networks calibrated by means of high-fidelity load simulations, Journal of Physics: Conference Series, 1037, 062 027, https://doi.org/10.1088/1742-6596/1037/6/062027, 2018.
 - Singh, D., Haugen, E., Laugesen, K., P. Dwight, R., and Viré, A.: Data-driven probabilistic surrogate model for floating wind turbine lifetime damage equivalent load prediction, https://doi.org/10.5194/wes-2025-24, 2025.
 - Snoek, J., Larochelle, H., and Adams, R. P.: Practical Bayesian Optimization of Machine Learning Algorithms, 2012.
 - Stehly, T. and Duffy, P.: 2020 Cost of Wind Energy Review, Tech. Rep. TP-5000-81209, NREL, Golden, CO, 2021.

695

700 Ucar, A. and Balo, F.: Assessment of wind power potential for turbine installation in coastal areas of Turkey, Renewable and Sustainable Energy Reviews, 14, 1901–1912, https://doi.org/10.1016/j.rser.2010.03.021, 2010.

- Vanem, E., Fekhari, E., Dimitrov, N., Kelly, M., Cousin, A., and Guiton, M.: A Joint Probability Distribution Model for Multivariate Wind and Wave Conditions, in: Volume 2: Structures, Safety, and Reliability, p. V002T02A013, American Society of Mechanical Engineers, Melbourne, Australia, ISBN 978-0-7918-8684-7, https://doi.org/10.1115/OMAE2023-101961, 2023.
- 705 Veritas, D. N.: Recommended Practice DNV-RP-C203 Fatigue design of offshore steel structures, Tech. rep., 2010.
 - Yamazaki, W., Rumpfkeil, M., and Mavriplis, D.: Design Optimization Utilizing Gradient/Hessian Enhanced Surrogate Model, in: 28th AIAA Applied Aerodynamics Conference, American Institute of Aeronautics and Astronautics, Chicago, Illinois, ISBN 978-1-62410-141-0, https://doi.org/10.2514/6.2010-4363, 2010.
 - Yildirim, B. and Dimitrov, N.: HIPERWIND D4.4: Floating wind turbine structural design procedure including SLS, Tech. rep., 2024.
- Yildirim, B., Dimitrov, N., Abrahamsen, A. B., and Kolios, A.: A reduced order/simplified method for uncertainty quantification on the floating wind turbine design basis, Journal of Physics: Conference Series, 2024.
 - Zhang, H., Wang, H., Cai, X., Xie, J., Wang, Y., and Zhang, N.: Novel method for designing and optimising the floating platforms of offshore wind turbines, Ocean Engineering, 266, 112 781, https://doi.org/10.1016/j.oceaneng.2022.112781, 2022.
- Zhang, X. and Dimitrov, N.: Variable importance analysis of wind turbine extreme responses with Shapley value explanation, Renewable Energy, 232, 121 049, https://doi.org/10.1016/j.renene.2024.121049, 2024.